Structural diversity and ecosystem-resource relationships in tropical savanna and a legume-cereal intercrop

Maged Ikram Nosshi

Submitted to the graduate degree program in Department of Geography and Atmospheric Science and the Graduate Faculty of the University of Kansas in partial fulfillment of the requirements for the degree of Doctor of Philosophy.

Committee members

David B. Mechem, Chairperson

Nathaniel A. Brunsell, Co-Chair

Kelly Kindscher

Timothy E. Crews

Jesse B. Nippert

Bryan Foster, External Reviewer

Date defended: February 4^{th}, 2019

The Dissertation Committee for Maged Ikram Nosshi certifies
that this is the approved version of the following dissertation :

Structural diversity and ecosystem-resource relationships in tropical savanna and a legume-cereal intercrop

David B. Mechem, Chairperson

Date approved: _____

Abstract

While the most productive ecosystems on Earth, correspondingly the most diverse, function within limitations of energy and resource flows, the general approach of high-yielding agriculture, in contrast, has been to simplify and replace key ecosystem functions with non-renewable inputs. Restoring ecological processes in agriculture requires some understanding of the underlying mechanisms. Here, I explore a unifying framework regarding the coupling between ecosystem structure and function. Namely, that the capacity of water-limited ecosystems to optimize water use, or resist stress is a product of their life-form diversity. I apply this hypothesis to infer the response of structurally contrasting ecosystems at a wide range of scales: (i) At the plot scale, I test the role of resource complementarity ("niche-based" mechanisms) in a perennial grain-legume intercrop, using stable isotope analysis. (ii) At the sub-continental scale, I use satellite data to explore the response of one of the most variable terrestrial biomes, tropical savanna, to rainfall variability. I employ different approaches to demonstrate the degree of coupling between ecosystem response and the environmental forcing. The dissertation concludes by summarizing the key findings and outlining further work needed to explore the role of ecosystem structure on function in water-limited systems. I discuss the implications of niche complementarity on resource relationships of biologically diverse agroecosystems, emphasizing the need for a re-evaluation of the conceptual framework used to envision niche complementarity to account for alternative resource acquisition pathways. I explore the role of savanna hydrophenology as a stabilizing mechanism, relating patterns of synchrony to savanna structure and composition. The relevance of this work is directly linked to

the loss of ecological function which manifests in agriculture's growing dependence on fossil energy to mask diminishing returns from extractive use of land and water resources. Enriched knowledge of potential mechanisms, coupling structural diversity with ecosystem function, in both natural and managed ecosystems, will provide insight into the ecological basis for diversity driven processes in water-limited ecosystems.

Acknowledgements

Many people helped make this work possible. To a large degree this dissertation has been an opportunity for me to learn ways of doing ecological research beyond what was familiar. For this I thank Nate Brunsell, my supervisor, for his engagement and guidance. I am grateful to Tim Crews for the opportunity to participate in meaningful ways in the ongoing work at The Land Institute; from the space to conduct field work with support from able staff, to feeling welcome and engaged. For the staff at TLI and the motivation behind the work I have great appreciation. Thanks to Stan Cox for first throwing the opportunity my way when I was in Egypt, and Ron Kinkelaar for his friendship and poker runs. For help making sense of stable isotope results and a lot of critical input throughout the study I am grateful to Jesse Nippert. Lawrence Sheppard with the Kansas Biological Survey was generous with his time, and whose knowledge of surrogate data testing was extremely helpful in conceptualizing the problem. Tarik Gouhier shared code for the surrogate data testing procedure, and Bernard Cazelles provided clarification on the merits of the approach as well as feedback on results. I would like to thank Skylar Koerner, Ferdouz Cochran, Jeff Delaroy, Kelly Logan, Suzy Satcher and Jian Yang for their help and distractions. Thanks to Bryan Foster, Daniel Hirmas, Kelly Kindscher and David Mechem for their willingness to share their time. Finally, Marisela Chavez made the last two years exciting and meaningful. With the support of my family I am enabled and encouraged to prioritize this work and see it through completion, while life goes on at the same time. Grateful to Marian Nosshi for her help in making this possible. The Rotary Club Field Research Grant of Topeka funded my first field season. The Mari F. Pesek Graduate Research Award

and Summer Research Research Fellowship provided funding for a follow-up field season. The final year of my PhD was supported by a fund from Malone Family Land Preservation Foundation and my work as a Research and Teaching assistant.

Contents

List of Figures

List of Tables

Chapter 1

Introduction

1.1 Introduction to the dissertation

This dissertation documents work across a wide scope of scales undertaken in entirely different ecosystems, both in managed and natural systems. Divided into three main parts: (i) At the plot-scale I determine the role of resource partitioning in a novel agroecosystem in Central Kansas, where a multifunctional, perennial grain polyculture is being developed. At the subcontinental-scale, spanning a precipitation gradient along the Kalahari sand sheet between Zambia, Namibia, Botswana and South Africa, I compare eight savanna varying in tree-dominance in terms of their response to variable rainfall. For (ii) I determine differences among savanna in their response sensitivities across different temporal scales. For (iii) I determine the degree of synchrony between savanna phenology (green-up) and rainfall onset, as an additional measure of how coupled versus buffered different savanna are from environmental variability.

No common ecological model encompasses this work, although some overlap of processes and mechanisms can be drawn out among the three studies. For example, niche partitioning is evoked in expanding agroecosystem water utilization, it is also central to equilibrium models ("bottom up" controls) used to help explain the successful coexistence of trees and grasses in tropical savanna. Nor is there a single context which determines the cohesion between these studies. However, water, but more generally resource acquisition might stand out as a common perspective across the three. A much broader common thread ties this work together: all three studies explore the coupling between ecosystem structure and function. This provides the background, objectives and motivation behind this work.

To place this work in context, it falls at the intersection of ecosystem and community ecology. At this scale of inquiry the physical environment is included, both as a an influence on, as well as an outcome of biological processes. By including community-level interactions, research into ecosystem structure and function is focused on understanding life's diversity. From processes explaining species coexistence, to the regulatory outcomes diversity has on ecosystem behavior and the capacity to mediate and respond to change. Where relevant I draw connections between what we can learn from diversity and ecosystem function to inform low input agriculture. An approach dependent on restoring ecological function in how we grow food, and most pertinent to limited resource conditions.

How ecosystem functional attributes are a product of ecosystem structure is explored in the role ecosphysiological differences play out in the acquisition of water from different sources when intercropping a legume and a perennial grain. Broadly, the question is whether a mixture can outperform single-species stands of a perennial grain, and in the case where their is overyielding, can this be attributed to complementary effects, and specifically, niche partioning over water sources? Because of the perennial nature of this developmental agroecosystem I expect these interactions to be a major determinant of their success, since they play out over a longer term than a single growing season, and likely to intensify with time. How ecosystem structural attributes determine response to variable rainfall is explored in one of the most unique biomes structurally, and interestingly the largest: tropical savanna. Along a precipitation gradient, where ecosystem response is not limited structurally, as vegetation composition and tree-dominance changes along the gradient, I determine differences among savanna in their sensitivity to variable rainfall at different temporal scales. To further explore how much regulation or homeostasis ecosystems posses, I determine the degree to which savanna green-up is coupled with rainfall onset as the degree to which they are synchronized.

In Chapter 2, I describe the research trials comparing single species plots of *Thinopyrum intermedium* (Kernza®) with diversified plots, intercropping Kernza with Medicago sativa (alfalfa), to explore the role of complementarity on productivity. I report results comparing the productivity of

the different treatments and relate that to the degree of source water separation between the grass and legume. Chapter 3 moves focus to the gradient study where I ask when are there differences in response patterns among structurally variable savanna across a 14-year record. This line of inquiry is picked up in Chapter 4 where I report on differences among the same savanna sites to determine the degree of coupling between savanna phenology and the timing of rainfall. Chapter 5 summarizes all the results and their implications with some paths for future work.

Chapter 2

Functional diversity and resource partitioning in a perennial grain agroecosystem

Abstract

While differences in resource access and use among species helps explain coexistence patterns, they also control the overall performance of the community. Using natural abundance of stable isotopes to track contributions from different sources of water we explore the importance of source partitioning in a functionally diverse perennial grain agroecosystem. Single species plots of *Thinopyrum intermedium* (Kernza®) displayed marked intraspecific competition, in contrast to overyielding measured in the diversified grass-legume plots, where intercropping Kernza with *Medicago sativa* (alfalfa) doubled total aboveground net primary productivity (ANPP), with no negative effects on grass productivity. Complementary effects were mirrored by distinct source water separation between the grass and legume. These findings are the first to report a vapor signature for xylem water with implications for expanding the existing framework with which resource partitioning is conceived. We suggest that in addition to the degree of niche overlap, resource partitioning should also consider the rare case of an alternative source of a resource.

2.1 Introduction

How a diverse ecosystem can perform relative to a simplified version of it remains to be a relevant question intersecting community- and ecosystem ecology. Developments around diversity-driven effects on ecosystem function have shifted emphasis from the role of species richness to a mecha-

nistic approach focusing more on species composition, emphasizing the role of life-form diversity (Hooper et al., 2002, 2005). While observations from experimental grassland communities found that both the number and type of species present are equally important in determining ecosystem function (Hector et al., 2011), results from experimental species assemblages conclude that a positive relationship with species richness and ecosystem function tends to saturate at low levels of diversity (Tilman et al., 1996; Hector et al., 1999; Chapin et al., 2000).

Ecologically-functional, biologically-diverse agroecosystems present an opportunity to explore the role of ecological mechanisms linking species diversity to ecosystem function. Perennial grain polycultures, consisting of high seed yielding mixtures of grasses and forbs, have been proposed for the Great Plains of North America (Cox et al., 2006). Positioned along a disturbance continuum between pastoral systems and low-input subsistence farming (Crews et al., 2016), perennial polycultures result in novel species interactions when compared with annual agriculture; exhibiting patterns of resource acquisition and use meant to approach those of the native ecosystem replaced and lasting beyond a single growing season. Where access to external inputs is not the reality of limited resource farmers, the potential of perennial grain polycultures to restore ecological function, in terms of resource acquisition and use, becomes more than an abstract interest. Where access to external inputs is an achievable luxury in a different socioeconomic reality, restoring ecological function in the acquisition and use of inputs can have a transformative effect, assuming aligned economic incentives (Liebman et al., 2008). Managing life-form interactions to address questions specific to resource acquisition and use, based on an understanding of the coupling between ecosystem structure and function is central to this effort.

Differences among species in the way they use a limiting resource, leading to higher overall productivity in mixtures relative to single-species stands are described by ecologists as complementary effects, and envisioned in terms of the degree of niche overlap (Wojdak & Mittelbach, 2007). In the hypothetical example of two species with high niche overlap (Fig. 2.1A) a change in species composition results in little to no change in ecosystem function. In contrast, with low niche overlap (Fig. 2.1B) a change in composition brings about a large change in ecosystem function (in

this case productivity).

Niche processes, including below ground resource partitioning, have helped explain the coexistence among grassland species. Suggestive evidence for the possibility of resource partitioning originally came from surveys of the vertical layering of roots (see Figure 40 Albertson (1937) and Weaver (1966); Sun et al. (1997)), but more recently confirmed to actually account for resource uptake with the use of stable isotope methods (Ehleringer & Dawson, 1992). Consistent differences in resource use among life-forms representative of the tallgrass prairie appear (Nippert & Knapp, 2007; Nippert et al., 2012). Warm season (C_4) grasses have been shown to be restricted to the surface depths, while shrubs and forbs, particularly C_3 forbs, exhibit more flexibility. Under dry conditions differences between life-forms become most pronounced and as C_3 forbs switch to deeper source water (Nippert & Knapp, 2007).

Absolute isotope values alone help link xylem water to source water, further insight into processes of affecting water isotope fractionation comes from exploring deviation from the Global Meteoric Water Line (GMWL) describing global precipitation water. Dual isotope plots ($\delta^{18}O$: δD) reflect changes in phase as water moves through the ecosystem. The ratio is highly sensitive to environmental temperature and humidity. The slope of the GMWL is a result of condensation in rain clouds consistently occurring under equilibrium conditions (100 % RH) between liquid and vapor. Equilibrium fractionation consistently results in a higher fractionation factor (α) for δD than $\delta^{18}O$ – exactly 8 times higher, which equates with the slope of the GMWL. Deviation from the slope of the GMWL results from evaporation. Evaporation under non-equilibrium conditions (RH $<$ 100%) results in a more depleted vapor (more negative relative to GMWL), and enriched residual water with a slope $<$8, resulting from a larger kinetic fraction factor for $\delta^{18}O$ than δD. Therefore, by considering the slope of the $\delta^{18}O$/ δD relationship we can understand more about processes, such as changes in phase, which water might have undergone.

Here we quantify the degree of niche overlap among species to determine the role of resource partitioning on ecosystem function in a novel perennial agroecosystem during the 2^{nd} and 4^{th} years of establishment. We tested the hypothesis that life-form differences in resource acquisition will

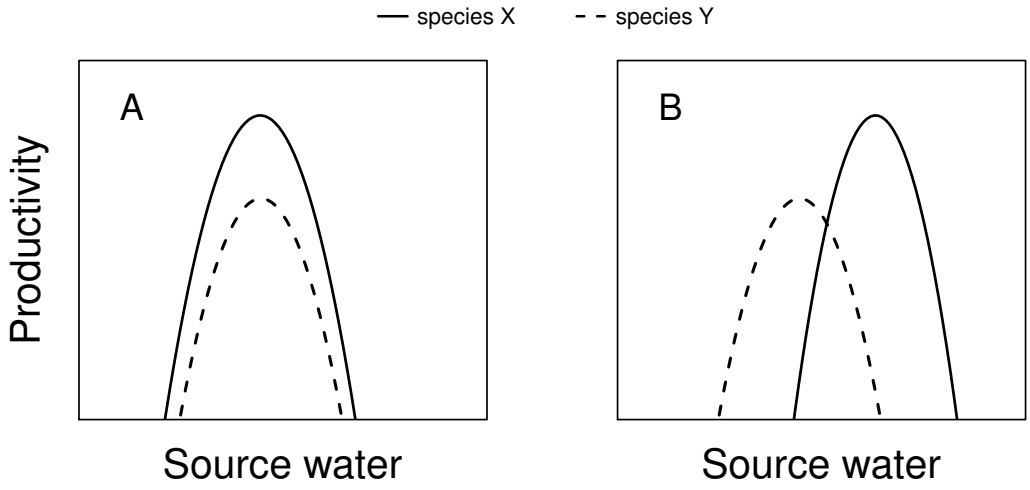

Figure 2.1: **The niche complementarity hypotheis suggests that differences among species in resource use, or phenology will result in increase ecosystem functioning.** The conceptual framework is based on different degrees of niche overlap (resource partitioning). (A.) Null-hypothesis, no effect of species diversity on ecosystem productivity; (B.) Complementary resource use resulting in increased community productivity.

have a complementary effect on community productivity when intercropping Intermediate wheatgrass (Thinopyrum intermedium–which produces Kernza®grain, breeding cycle 2) with *Medicago sativa* (alfalfa, I-70). Specifically, we tested the partitioning of water sources by life-form. We present a case which calls for expanding the existing framework around complementary effects (Fig. 2.1) to consider the role of alternative sources of a resource. While this is not novel in general, it is in the particular case of water, as discussed further.

2.2 Methods

2.2.1 Study plots

We explore resource acquisition and use of a perennial grain in different diversity and planting density arrangements, using field trials that began at the Land Institute (38°46'8"N, 97°33'8"W) in the Fall, 2012. Kernza was sown in single-species plots and intercropped with the N-fixing legume, alfalfa (*Medicago sativa*), a perennial legume with a water consumption range widely adaptable to high consumption as well as an ability to perform under deficit (Zhang et al., 2006; DePeters, 2012). Single-species plots were replicated at two densities: (1) narrow spacing (KK), sown at a 38 cm row spacing, and (2) wide spacing (K), sown at a 76 cm row spacing, compared to a functionally diverse treatment (3) where Kernza at wide spacing was intercropped with alfalfa (KA) in alternating rows. Treatments were randomly assigned to 4 plots for a randomized complete block design. We included a high nitrogen fertilizer treatment (150 kg N ha^{-1} + 20 kg P ha^{-1}, KK+NP) for reference, representing the yield response when N is not limiting plant growth (considering $>$ 150 kg N ha^{-1} are removed in harvest as well as sequestered in an aggrading soil organic matter pool in this perennial agroecosystem, unpublished data).

2.2.2 Plant water status

We measured leaf water potential weekly for each of the three treatments: K, KK, and KA. Measurements were done in the field using a Scholander pressure chamber (Soil Moisture Equipment

Corp, Santa Barbra, CA), at mid-day (Ψ_{md}) and pre-dawn ((Ψ_{pd}) during peak growing season (June-July). We excised the youngest fully expanded leaves with a razor and secured it in the pressure chamber, and recorded the pressure when xylem water emerged from the cut section.

2.2.3 Isotope sampling and analyses

To link plant xylem water with source water we collected monthly samples between May and July in 2014, for all the treatments (k, KK, and KA, both Kernza, alfalfa and soil were sampled) and June through August in 2016, (only alfalfa, dew and deep soil water sampled). Any approach involving destructive sampling of water isotopes is only representative of a snap shot in time. We sampled during early spring and again in mid summer. To represent peak plant uptake, we collected plant water samples during mid-morning, when evaporative demand was low and transpiration rates close to maximum to avoid periods of water stress or wilting. On each date we collected a single 5 cm soil core by hand, down to a meter depth, and divided into increments using a sectioned plastic sleeve inserted inside the corer. Adjacent to each core, we harvested two individual plants for xylem water; crowns, in the case of Kernza, and coarse roots, in the case of alfalfa (following (Thorburn & Mensforth, 1993)). All plant and soil samples were sealed inside 12 ml Exetainer vials (labco, UK), placed on ice until transported to the laboratory where they were kept frozen until extraction.

Data from 2014 suggested that alfalfa accessed a highly depleted source outside of our sampling range. Therefore in 2016 we sampled deep soil water and dew to consider alternative source water and the possibility for foliar uptake. Dew samples were collected at dawn on a glass pane mounted at a 45° angle within the canopy. We collected soil samples down to a 4 meter depth at 1.2, 1.8, 2.4, 3 and 4 meters, using a Geoprobe hydraulic direct push probe (Geoprobe systems, Salina, KS). Assuming that the isotopic composition of deep soil water pool is rather stable over time and least affected by surface processes we collected deep soil samples in a mowed grass alley immediately adjacent to the sampled plots to avoid disturbance.

Finally, we calculated the local meteoric water line (LMWL) using data from the Konza Prairie

(90 km E/NE) from monthly measurements of rainfall over an 13-year record (2001-2013).

We extracted and analyzed soil and plant samples for δD and δ^{18}O at the Stable Isotope Mass Spectrometry Laboratory of Kansas State University. Accordingly, xylem and soil were extracted water using cryogenic vacuum distillation (Ehleringer & Osmond, 1989). Samples were then analyzed for stable isotopic composition using a Picarro WS-CRDS isotopic water analyzer, and ChemCorrect software to identify possible sample contamination. Values are expressed as deviations from Laboratory standards, calibrated to Vienna Standard Mean Ocean Water (VSMOW, δD and δ^{18}O). Overall, measurement uncertainty of the analyzer was <1‰ for δD and <0.3‰ for δ^{18}O.

2.2.4 Statistical analysis and source water contribution

All data were tested for departures from normality using Shapiro-Wilk's test, and visual inspection of Kernel density and Q-Q plots. The 3 planned comparisons of treatment effects on ANPP (K:KK, K:KA, KK:KA) were done using pairwise t-tests with no corrections for multiple comparisons. Two sample t-tests were used to test for a seasonal effect on the isotopic signature of xylem water between spring and late-summer.

We determined the likely contribution from different source water to plant water uptake by fitting a Bayesian mixing model using the MixSIAR framework (Stock & Semmens, 2016a). Based on a dual-isotope plot (δ^{18}O vs. δD) of all potential source water sampled, we considered three sources and divided by soil depth: 0-5 cm, 5-30 cm, 30-120 cm. We did not consider dew as a source contributing to Kernza water uptake because it had a distinctly more enriched signature than xylem water. We modeled spring and late summer separately to evaluate the effect of season on source water contribution, with season as a fixed effect and no prior information. Model error structure was based on residual errors only, assuming unknown sources of variability, or "process errors" based on chance alone (Stock & Semmens, 2016b). Model parameters were as follows: chain length = 100,000, burn = 50,000, thin = 50, number of chains = 3.

2.3 Results

2.3.1 Total ANPP

To evaluate the treatment effect (K, KA and KK) as an outcome of competition and resource use rather than planting density multiplied Kernza ANPP in the high density plot (KK) by a factor of 0.5. Doubling planting density from 76 cm spacing (K) to 38 cm (KK) had no net effect on total ANPP (P = 0.973), but a negative effect on Kernza ANPP (P = 0.025). Kernza ANPP decreased by 49.4% in the higher density plot(Fig. 2.2). On the other hand, intercropping the legume with Kernza doubled total ANPP by the 3^{rd} year of establishment (P = 0.006) (Fig. 2.2, A), with KA at 9146 kg ha^{-1} $\pm$ 860 SE, matching the fertilized treatment (KK+NP). Intercropping Kernza with alfalfa had no negative effect on Kernza ANPP (KA:K, P = 0.851) (Fig. 2.2, B). The incorporation of the legume therefore doubled the ANPP of the entire system at no cost to the productivity of Kernza. Together, this suggests the existence of high intraspecific competition within Kernza and complementary interactions between Kernza and alfalfa.

2.3.2 Isotopic analysis of xylem and source water

Kernza and alfalfa used different water sources. Kernza xylem water closely matched the isotopic composition of soil water; enveloped entirely within the signal range of soil water collected at different depths down to 4 meters (Fig. 2.3). Xylem water from alfalfa, on the other hand, shows access to a source we did not sample (Fig. 2.3), falling entirely outside the range of soil water down, or dew. To verify that this was a real and consistent effect we sampled alfalfa over different years (2014 and 2016), across different seasons (May - August), for different establishment age (2-year and 4-year alfalfa), and in a neighboring field trial established in 2014 (Fig. 2.3). Consistently, alfalfa signaled a highly depleted signature of a vapor source.

Season did not have a pronounced effect on the mean isotopic signal of Kernza xylem water (t = 1.7389, df = 23.901, p-value = 0.0949). In contrast, alfalfa xylem water became more depleted going from spring to late summer (t = 3.6917, df = 9.1901, p-value = 0.0048) (Fig. 2.4)

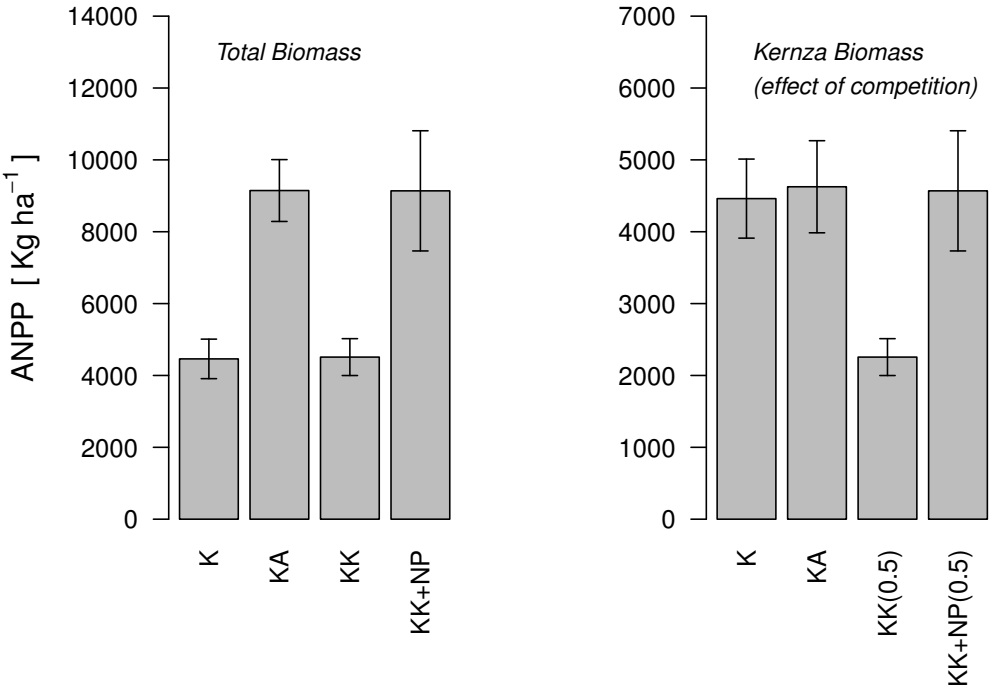

Figure 2.2: **Functional diversification and productivity.** (left) Mean total ANPP (+1 SE) during the second growing season, 2014, for 3 treatments: (K) single species wide spacing, (KA) Kernza-alfalfa intercrop, (KK) single species narrow spacing. (right) The effect of competition on mean Kernza ANPP (+1 SE). Note, to isolate the effect of treatments on Kernza productivity, through intraspecific competition (KK) and interspecific competition (KA), we multiplied Total ANPP by (treatment spacing/76 cm). In the case of wide spacing (K) and the intercrop (KA), Kernza spacing is 76 cm, therefore the factor = 1. In the case of narrow spacing (KK and KK+NP), Kernza spacing is 38 cm, therefore the factor = 0.5 (marked on x-axis labels). Intercropping (KA) doubled total aboveground biomass, with no effect on Kernza biomass, in contrast to intraspecific competition observed in the single species treatment (KK).

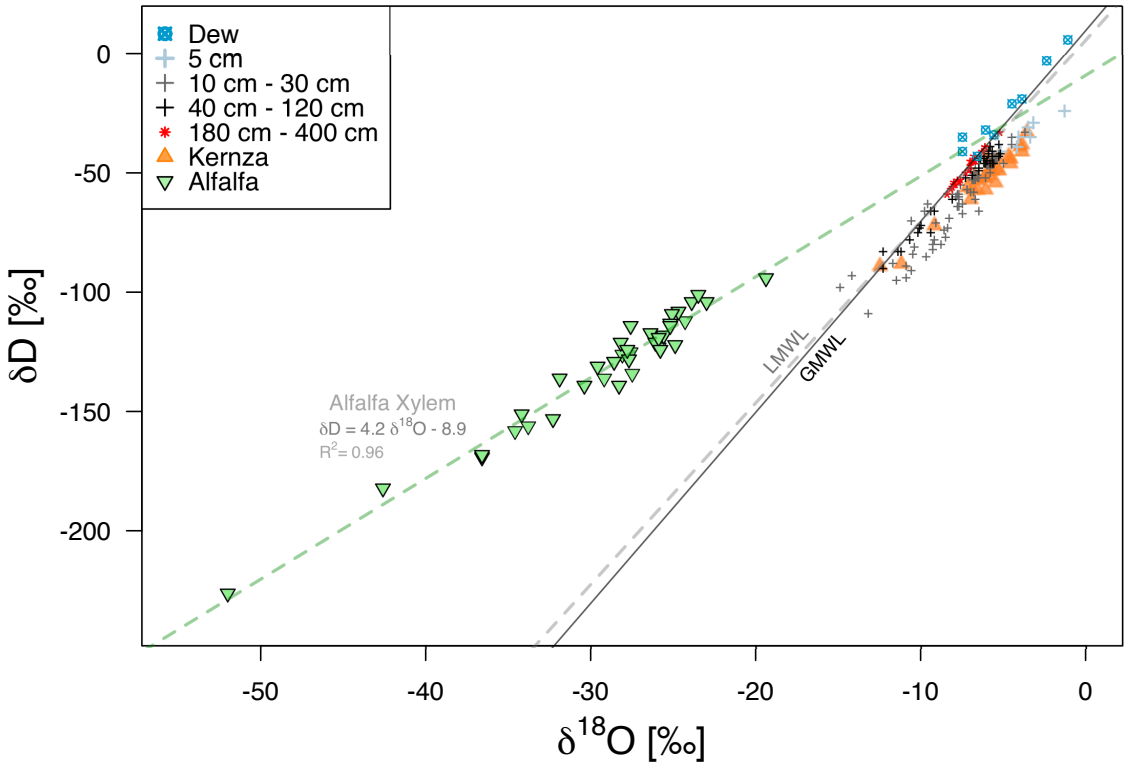

Figure 2.3: **Dual isotope plot for delta-D and delta-18O of xylem water for alfalfa and Kernza, deep soil water at different depths and dew.** Alfalfa xylem water (green triangles) falls on the same line for 4th year alfalfa and 2nd year alfalfa, as well as alfalfa sown in a neighboring field.

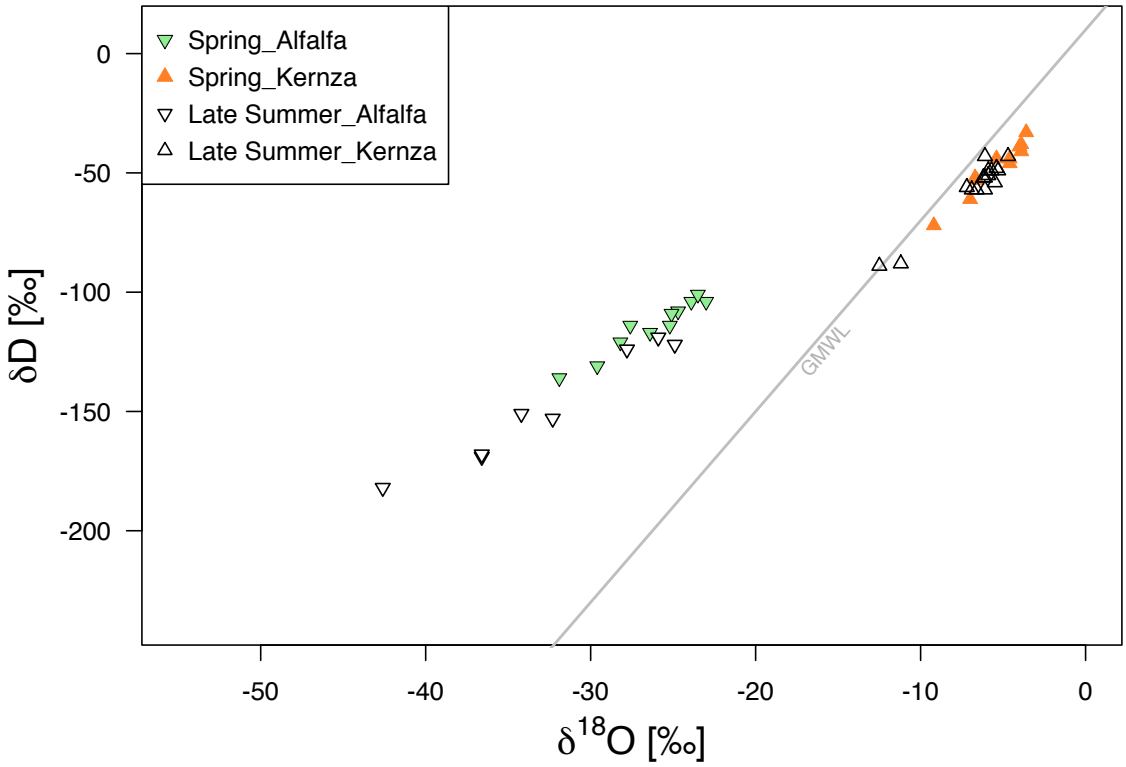

Figure 2.4: **Delta-D and delta-18O of xylem water for alfalfa and Kernza.** As the season progressed alfalfa showed a significant seasonal effect, becoming more depleted going from spring to late summer. Kernza showed a similar pattern but not as pronounced.

For a more detailed analysis of soil water isotopes we intensively sampled and analyzed 13 depths (5, 10, 15, 20, 25, 30, 40, 50, 60, 70, 80, 90, 100 cm) in the KK treatment, in comparison to only 3 depths (10, 30, 80 cm) in all other treatments. Two way analysis of variance showed no seasonal differences in soil water isotope composition (p-value = 0.69510), but a significant difference by depth (p-value = 0.00571). This was a result of the top 5 cm being consistently more enriched in heavy isotopes (δD and δ^{18}O) than all other depths (Fig. 2.3). Dual isotope ratio of deep soil water, between 1.8 m - 4 m, was highly constrained and fell directly on the GMWL (Fig. 2.3), which suggests a direct link with meteoric water.

2.3.3 Mixing models and Kernza source water

Kernza used water from different depths depending on the season. In spring 45.8% came from the top 5 cm, 22.4% between 10-30 cm and 31.8% from deep soil water (between 40-120 cm). In late summer the contribution from the surface soil water was much less important compared to spring, with 15.7% from the top 5 cm, 50% from 10-30 cm, and 34.3% coming from deep soil water, 40-120 cm depth.

To probabilistically estimate the contribution of multiple sources to a mixture using Bayesian implementation of mixing models all sources must be sampled. At this point we are unable to estimate contributions by source to alfalfa without sampling the vapor source which alfalfa is accessing.

2.4 Discussion

Intercropping alfalfa with Kernza doubled aboveground biomass with no sign of interspecific competition with alfalfa. In contrast, strong intraspecific competition was observed in the KK treatment. Stable isotope analysis of xylem water suggests that the two species utilize water sources of very different signatures. Kernza matching closely the soil water sources sampled. In line with studies of nearby native Tallgrass species, Kernza exhibited a seasonal shift in source water contri-

butions (Nippert & Knapp, 2007). However, in contrast to warm-season grass species (Nippert & Knapp, 2007), Kernza's dependence of deep soil water increased as the growing season progressed and soil water at surface depths dried up. In contrast, both warm-season grasses and cool-season forbs relied proportionally less on deep soil water in July and August (Nippert & Knapp, 2007). Also notable is how deep soil water, regardless of season, represented a proportionally larger contribution to Kernza water uptake than it did in the case of Tall grasses (between 30-36% in the case of Kernza, compared to an average of 12% for warm-season grasses and 23% for cool-season forbs (Nippert & Knapp, 2007)).

Isotope composition of alfalfa xylem water, on the other hand, indicates access to a highly depleted (light) source, suggestive of a vapor source. Consequently, dew water was sampled in 2016, along with soil water at upto a 4 meter-depth (30 cm, 120 cm, 180 cm, 240 cm, 300 cm, 400 cm)and compared with plant alfalfa, and Kernza xylem water.

In the rare case where source waters do not match the range of δD and δ^{18}O of xylem water there is the possibility of fractionation of water taken up by roots. Reports of fractionation have been largely linked to when water uptake is an active process, symplastic, as observed in coastal wetland species (Lin & Sternberg, 1993), and in xerophytic plants growing in arid envrionments (Ellsworth & Williams, 2007). In all reports of plant water fractionation during active uptake discrimination against deuterium is on the order of 3‰ to 10‰. Oxygen isotope ratio composition in such cases, however, match source water. While the pathway explaining deuterium discrimination of root water uptake has not been resolved, a credible explanation provided by Lin and Sternberg (1993) for the δD and δ^{18}O discrepancy is the disassociation of hydrogen bonds during water passage through membranes (Schönherr & Schmidt, 1979). While this explains discriminatory plant uptake against deuterium, it does not explain the depletion of ^{18}O we observed in alfalfa xylem water.

2.4.1 Foliar uptake of vapor vs. dew

Plants can take up water directly over their entire surfaces. Commonly, the majority comes from soil water, through the roots. The uptake of vapor sources of water by plants can take two thermodynamically different pathways. Water vapor absorbed by a hygroscopic surface inside a leaf is driven by the water potential gradient, while water vapor that condenses on a plant surface releases latent heat and the rate of condensation becomes limited by the rate at which this heat is removed, or a heat sink (Monteith, 1963). Therefore, there is a range of conditions under which foliar uptake might prove physically possible. At the wilting point, conventionally defined at -1.5 Mpa, leaves can absorb vapor from an atmosphere with relative humidity $> 99.8\%$ (Slatyer, 1958). It follows that the importance of foliar hydration can vary with environmental conditions, and has been shown to vary geographically within a given biome (Limm & Dawson, 2010).

Foliar absorption has been shown to be more important than previously appreciated, and particularly important under conditions of water stress (Breshears et al., 2008). The significance of foliar uptake of alternative water sources such as small rain events, fog, dew and vapor (Breshears et al., 2008; Dawson, 1998; Limm et al., 2009; Berkelhammer et al., 2013) has important implications for defining bioavailable water, with significant implications for survival limits. As an adaptive strategy, foliar absorption does not only allow plants to bypass soil water uptake, it also represents access to a more consistent water source. For example, in this region of the US dew occurs $>80\%$ of days during the peak growing season (Welp et al., 2008). However, considering these general relationships and comparing the water status of alfalfa throughout the growing season, which hardly drops below -1.5 Mpa (Fig. 2.5), makes foliar uptake of vapor a less than likely explanation of alfalfa source water in this study.

2.4.2 Separate soil water pools

Among the first surprising observations employing stable isotopes to link plant water uptake to source was Dawson & Ehleringer (1991) showing that mature stream side trees did not rely on stream water. More recently, the idea that plant roots take up water from a completely mixed soil

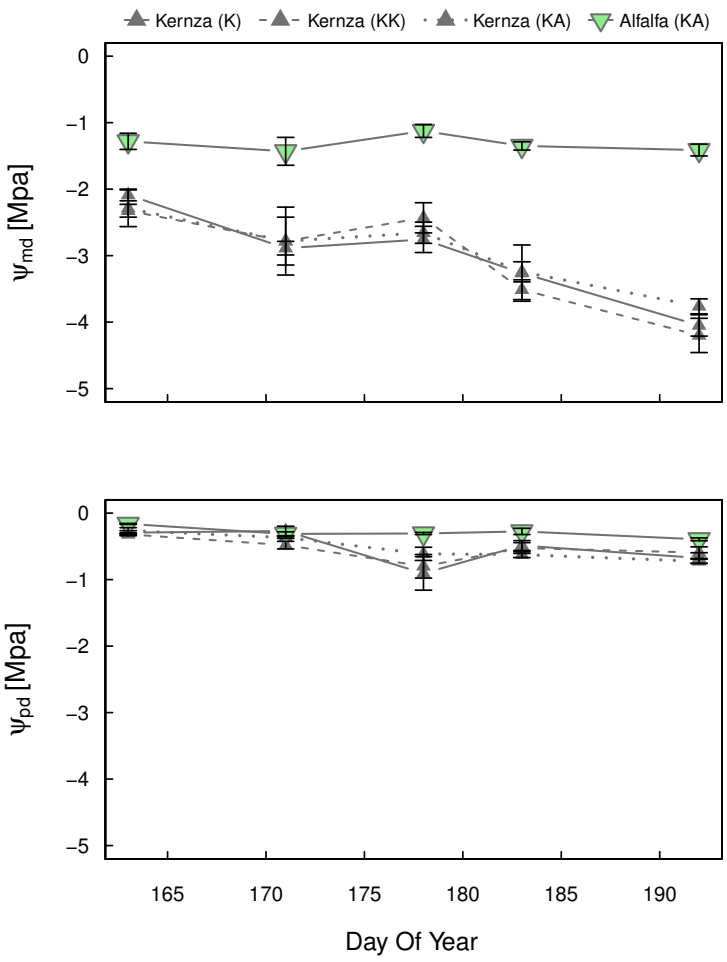

Figure 2.5: **Leaf water potential** (measured at midday, predawn) of Kernza (grey triangles) and alfalfa (green triangle) as a function of day of year, separated by treatment (K: single species wide spacing, KK: single species narrow spacing, and KA: Kernza, alfalfa intercrop). Data represent the mean $\pm$SE (n = 4 plants per treatment). Alfalfa maintains a relatively high leaf water potential (mostly above -1.5 Mpa) while Kernza shows more sign of water stress (top) as the season progresses.

water pool has been challenged (Brooks et al., 2010), with evidence that mobile water shares the same isotopic signature as meteoric water (eg.: rain, fog, dew, snow) while tightly bound water within small pores – bulk soil water – will plot along a soil evaporation line (Brooks et al., 2010; Sprenger et al., 2016; Hervé-Fernández et al., 2016). This poor and incomplete mixing of soil water does not explain our observation of a vapor signature for alfalfa xylem water, but it allows for the consideration of a bulk soil water pool to behave differently from the rest of soil water, and undergo changes in phase separately. But this does not explain the depleted vapor-like signature for alfalfa, falling to the left of the LMWL (Fig. 2.3)

For our observed alfalfa xylem water values to fall on a slope of $\sim$4 to the left of the LMWL it requires an equilibrium fractionation factor (α) much lower than the well defined slope for liquid-vapor fractionation of surface water, where equilibrium fractionation results in a slop of $\sim$8 (Horita & Wesolowski, 1994). Laboratory trials with proxy soils show an adsorption isotope effect that results in equilibrium isotope fractionation lower than those for surface water Lin et al. (2018), and with α values decreasing with decreasing RH. For the three trial soils with varying chemistry and pore sizes $S_{eq} = \ln \alpha(\delta D\text{-}\delta^{18}O) \sim 4$ - 7. While this explanation helps understand how soil water might have an isotope composition similar to vapor it still does not explain how alfalfa xylem water does not match any soil water sources we sampled.

2.4.3 Implications and future work

Regardless of the mechanisms explaining the depleted signal for alfalfa xylem water, which remain to be determined, life-form diversification in this novel agroecosystem resulted in a marked effect on ecosystem function, with total ANPP doubled. Our consistent observation of a depleted vapor signature for the legume regardless of establishment year, season, or plot location suggests access to an alternative water source not available to the grass. Consequently we believe that this might be a rare but important case where the existing framework for envisioning resource partitioning should be expanded. In addition to the two scenarios describing niche differences based on degrees of overlap (Fig. 2.1 A and B) we add a third scenario to the framework which considers an alternative

source. The third scenario (Fig. 5.1 C) describes a situation of resource use, where one of co-occuring species has access to an alternative source inaccessible to the rest.

The novelty of this finding, specifically a highly depleted, vapor-signature for plant xylem water, calls for further verification. On the one hand, there is consistency in our results when compared across the growing season, among different years, and even across different sites for alfalfa plots with different establishment years. Further support comes from the dual isotope plot ($\delta^{18}O : \delta$D), showing very little variability across all samples from the $\delta^{18}O : \delta$D line (Fig. 2.3). Such a predictable pattern is less likely when results are an artifact of noise or contamination, when we might see a less predictable pattern. Finally, the capacity for alfalfa to maintain such a stable plant water potential also suggests a biological relationship. On the other hand, errors due to contamination using isotope ratio infrared spectroscopy (IRIS), as in our analyses, are also very real (Brand et al., 2009; West et al., 2010).

2.5 Conclusions

Complementary effects resulting from resource partitioning proved important in a functionally diverse agroecosystem. Intercropping with alfalfa doubled total ANPP relative to the single species plot, at no cost to the grain crop, Kernza. This result we attribute to the legume's access to a water source which is not available to the grass. This level of niche partitioning along a limiting resource has implications relevant to ecology and how resource partitioning is commonly envisioned. It is also relevant for the diversification of agriculture and the capacity restore ecological function in how we produce food, going beyond increased yield. Multipurpose, biodiverse agroecosystems are perhaps most relevant to subsistence level farming, providing options for limited resource farmers. While this study constitutes a field trial of a developmental crop, the results are cautiously promising.

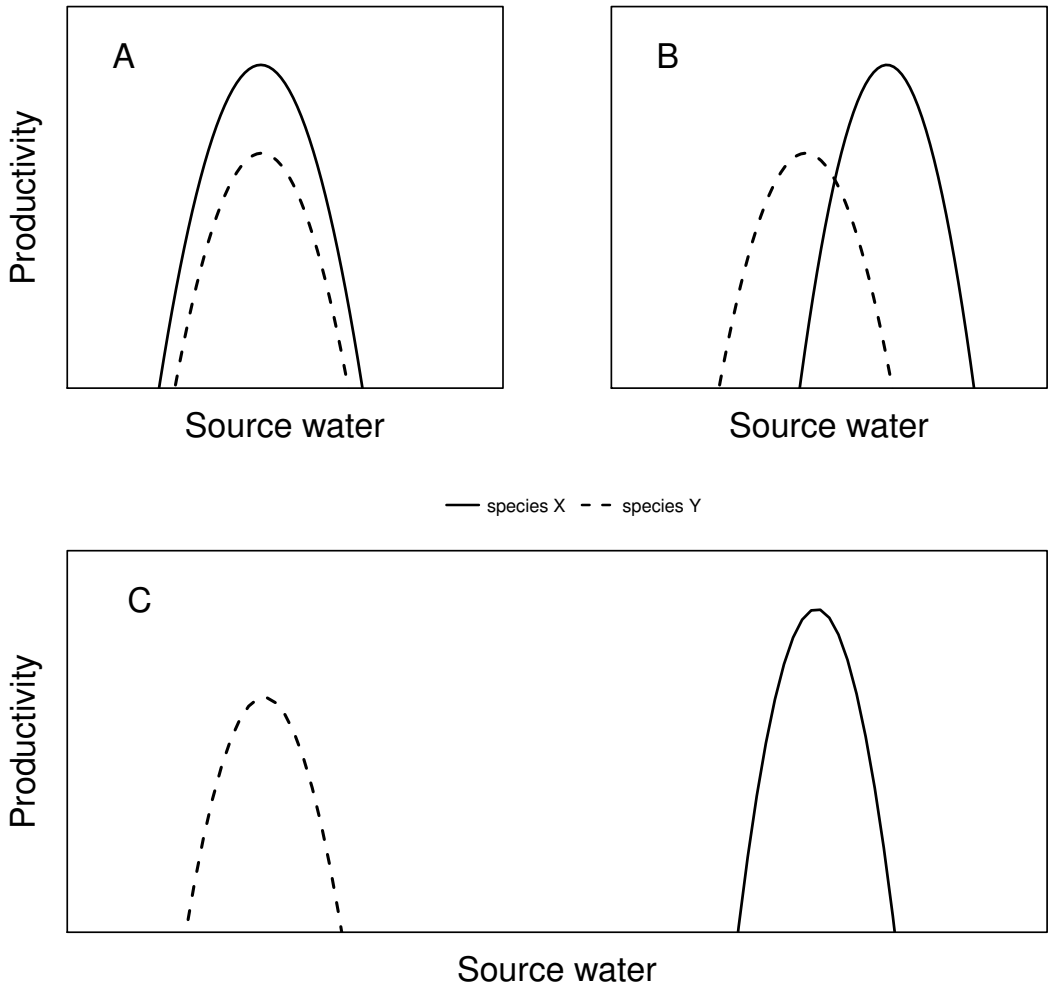

Figure 2.6: **Expanded conceptual framework for diversity-productivity relationships involving two species with varying degrees of overlap in niche space**. (A.) Null-hypothesis, no effect of species diversity on ecosystem productivity; (B.) Complementary resource use resulting in increased community productivity; (C.) A positive effect of complementary resource use involving an alternative water source.

Chapter 3

Ecosystem response patterns to rainfall variability in water-limited savanna

Abstract

Trees and grasses occupy contrasting functional groupings based on life history traits. The role of community structure in regulating ecosystem response in water-controlled systems is expected to change along resource gradients. At high water availability woody species utilize a larger portion of the water budget, highlighting biotic control. In more xeric climates, water availability likely dominates ecosystem dynamics regardless of structure. Ultimately, we expect tree-dominated savanna at the wetter end of the gradient to better moderate environmental fluctuations. We assessed response patterns of water-limited savanna to rainfall variability across a regional gradient using 14 years of satellite data for Enhanced Vegetation Index (EVI) and daily precipitation. We applied spectral analysis to decompose the response signal (EVI time-series) and determine differences in savanna sensitivity across time scales, and capture significant transient effects. Savanna types responded differently to rainfall variability, closely tracking changes in the relative contribution of trees and grasses. At ca. 600 mm of mean annual precipitation savanna diverge: below this point mixed tree-grass *shrubland-* and *wooded grassland* savanna are sensitive to the annual and seasonal fluctuations, and above it tree-dominated *woodland* savanna are responsive at the annual time-scale. The 600 mm isopleth also marks the peak for maximum grass biomass along the transect, below which water limits grass production and beyond it trees dominate. Seasonal lag effects also indicate the shortest response occurs at the center of the gradient, with the wettest and dri-

est savanna being the least responsive to seasonal fluctuations in rainfall. Sensitivity to extreme rainfall conditions (the wettest and driest years) reveals sharp differences along the transect: a $\pm$40% relative anomaly in precipitation resulted in a comparable response in EVI for *shrubland*- and *wooded grassland* savanna between 270 mm and 515 mm, compared to a 5% to 10% response for the wetter region between 638 mm and 791 mm *woodland* savanna. Also, annual precipitation extremes rarely coincided with the highest or lowest ecosystem response, suggesting a contextual response to rainfall events.

Our findings reveal a close coupling between ecosystem structure and function at the regional scale, with distinct differences among savanna in their sensitivity at different temporal scales. These differences aligned with different capacities to buffer the direct effect of rainfall variability.

3.1 Introduction

A few general principles can be drawn from the study of the relationship between biological diversity and ecosystem functioning (National Research Council, 2001). Much less is known about the degree to which ecosystem response patterns are coupled to community attributes, including their composition and structural diversity (Gherardi & Sala, 2015). How ecosystems respond to natural variability has been an ongoing area of research, with growing interest in discerning the direct effect of the physical environment from the moderated response which accounts for some degree of homeostasis. Of the initial syntheses from Long-Term Ecological Research (LTER) sites Knapp & Smith (2001) observed that most biomes considered exhibited an asymmetric response pattern to variable rainfall, such that the positive response to above-average annual rainfall was appreciably and consistently greater than the negative response to below average rainfall. They attributed this to an inherent capacity of natural ecosystems to buffer the direct effect of rainfall variability.

Drylands research constitutes an important contribution to the exploration of diversity-stability relationships. A component of the broader discipline of biological diversity-ecosystem function, focusing on interactions between ecosystem composition and the capacity to moderate the direct effect of the environment (Hallett et al., 2014). Drylands are anticipated to be the most sensitive

biomes to changing precipitation regimes (Weltzin et al., 2003). They are also frequently located where high interannual precipitation variability is experienced (Feng et al., 2013; D'Odorico & Bhattachan, 2012). Within drylands, where water rather than radiation or temperature controls energy flow (Noy-Meir, 1973), tropical savanna provide a unique opportunity to explore the coupling between ecosystem structure and response to environmental fluctuations. They are structurally unique, with contributions to net primary productivity shared between a mixed life-form of woody and herbaceous species, and are characterized by a highly seasonal climate.

Independent observations across drylands suggest that a diversity-stability relationship needs to consider interactions with historical environmental constraints on the performance of ecosystems in the face of fluctuations. For example, forest communities associated with drier localities were seen to better cope with drought anomalies, in a pattern that was positively linked to their diversity (Lloret et al., 2007), compared with more mesic environments, where there was no clear diversity-stability relationship. African savanna are some of the oldest biomes, their biota stand out among the most differentiated communities, having had a long evolutionary history uninterrupted by glaciation events (Walker, 2001). Significant differences in response to annual rainfall have been noted for different savanna regions (Ratzmann et al., 2016). Higher rainfall variability common to the Kalahari sand sheet compared to the Sahel region was attributed to a markedly higher response range in the Kalahari savanna, during both above and below average years (Ratzmann et al., 2016). Therefore, it is likely that for communities where high variability is common, a greater capacity exists in their response range.

The question of what makes ecosystems stable, versus fluctuate relative to environmental variability continues to be explored and the concept redefined. Past discord around the stability debate had largely been an issue of semantics (Doak et al., 1998) and the different ways "stability" can be used. One practical step to contribute to the development of unifying theory around stability are measurable indices. Avoiding some of this confusion we chose to follow the simple definition of stability as the ratio between the mean response and its standard deviation (Hallett et al., 2014).

Intuitive notions of the relationship between precipitation variability and ecosystem response

are likely to be challenged by several factors. In particular is an inconsistent response at different temporal scales, which includes two aspects of complexity: the first aspect (1) is the fact that conclusions about ecosystem response can be different depending on the temporal resolution of the data. To demonstrate (1), Williams & Albertson (2005) show that carbon flux differed during wet periods among savanna with different tree to grass co-dominance. However, when integrated over the annual time-scale, these structural differences did not have a lasting effect. At the annual time-scale water limitation was more important than structural differences among savanna (Williams & Albertson, 2005). Therefore, the time-scale of choice can lead to different conclusions about the importance of ecosystem structure.

The second case (2) is the contextual nature of events sufficient to trigger an ecosystem response. To demonstrate case (2), Adler & Levine (2007) observed that single year rainfall did not impact species richness in mixed-grass prairie, nor did consecutive wet years. Rather, species richness was most sensitive to a specific combination of wet and dry years (Adler & Levine, 2007) – when wet years followed a dry year. This highlights the significance of the contextual nature of the impact as a result of the interactive effect between current and previous year precipitation. Therefore, it is important to consider events, including extreme events, in the context of previous years.

Ecosystem response to rainfall variability is different over space and time. Looking specifically at ecosystem production, the spatial relationship with mean annual precipitation (MAP) is much stronger than the temporal relationship (Lauenroth & Sala, 1992; Williams & Albertson, 2005). In the short term, the temporal relationship is “structurally limited". In other words, productivity is limited by the pool of species present.

Regression approaches have been used to study the sensitivity of ecosystem response to fluctuations in the environment, with very useful insights from continental scale, or cross-site comparisons (Hsu et al., 2012; Good & Caylor, 2011; Ratzmann et al., 2016; Cleland et al., 2013; Hallett et al., 2014). Bearing in mind how ecosystem productivity and rainfall variability are related in more complex ways, here we re-examine the question of ecosystem sensitivity to variable rainfall

with wavelet analysis to capture transient effects. Similarly when we compare the response of the 8 sites to anomalous years we allow the response year to occur on different years from when rainfall was highest or lowest. Our motivating question is to determine how a structurally diverse biome responds to rainfall variability. We explore this for a regional resource gradient across the Kalahari sandsheet (Fig. 3.1a), with comparable rainfall variability (Fig. 3.1c), but where the relative contribution of herbaceous and woody life-forms changes (Fig. 3.1b). If the capacity to respond to environmental variability is to some degree a product of functional diversity; both in terms of the diversity of types (e.g. trees, shrubs, grasses), and their individual response range (Walker, 2001); then we expect interactions with climate variability to occur at different ecologically relevant timescales for different savanna types (Table 3.1) (Scanlon et al., 2005).

3.2 Methods

3.2.1 Sites

Africa marks a continent where water limitation defines much of savanna ecology (Sankaran et al., 2005; Good & Caylor, 2011; Bucini & Hanan, 2007) and where savanna – described as the non-adhering “pastor child of ecology", challenging classical ecological theory around competition (Scholes, 2016) – are the most extensive biome, covering almost half of the continent. The Kalahari Transect (KT) was chosen for its strong south to north rainfall gradient, across relatively homogeneous sandy soils and largely flat topography. Eight savanna sites were selected within a water-limited range between 270 mm - 791 mm of mean annual precipitation (MAP, Fig. 3.1), following Scholes et al. (2002). The southern most site marks the extent of the KT, at 27.75° S. The wettest site, at 16.75° S, still falls within a water-limitation range (Scanlon, 2003), with a distinct dry season spanning at least 6 months. The vegetation’s floristic and structural attributes for the area between 10° S and 29° S are well documented by Scholes et al. (2002).

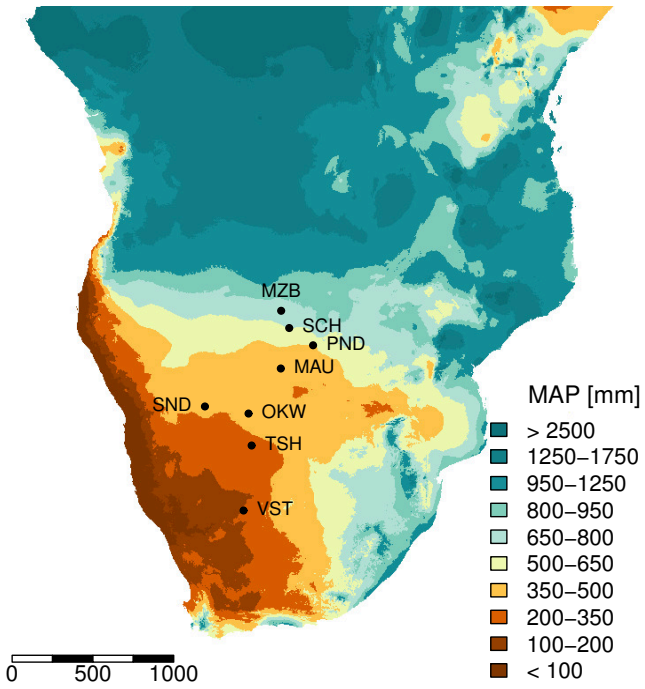

(a)

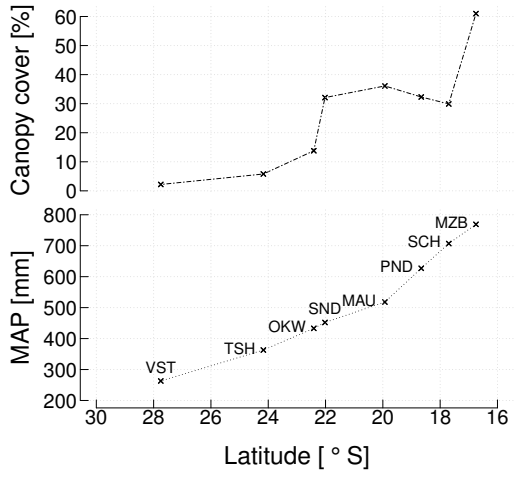

(b)

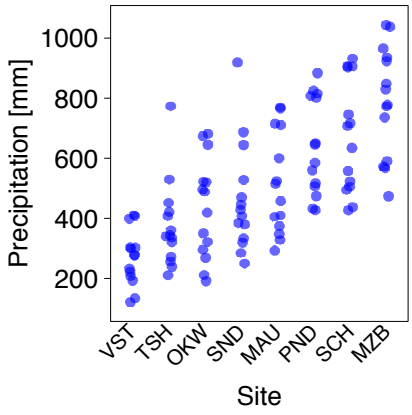

(c)

Figure 3.1: (a) **Study sites across a regional precipitation gradient**, ∼1 km resolution [data from worldclim.org]. (b) Woody vegetation cover and site location with respect to latitude and Mean Annual Precipitation (MAP). Canopy cover was estimated as the length of line segments with crown overhead on a 1200 m line transect for trees, and a 300 m line intercept for shrubs, data from (Scholes et al., 2002). (c) TRMM-derived annual precipitation range between 2003-2016 hydrological year. Note a comparable rainfall range across sites, save for a high anomaly year in 2006 for SND and TSH. Site abbreviations listed in Table 3.1

Table 3.1: **Characteristics of 8 savanna sites used in the analyses of EVI.** Three-letter abbreviations match the text and figures. Means for annual precipitation (MAP) are determined for the length of record observed between 2001-2014, while vegetation classification is based on (Scholes et al., 2002).

Site	Latitude	Longitude	Vegetation type	MAP (mm)
Maziba Bay Forest (MZB), Zambia	16.75 S	23.61 E	*Miombo* woodland	791
Sachinga Agricultural Station (SCH), Namibia	17.70 S	24.08 E	woodland	671
Pandamatenga Agricultural Station (PND), Botswana	18.66 S	25.05 E	woodland	638
Harry Oppenheimer Okavango Research Centre, Maun (MAU), Botswana	19.93 S	23.59 E	woodland	515
Sandveld Research Station (SND), Namibia	22.02 S	19.17 E	wooded grassland	463
Okwa River Crossing (OKW), Botswana	22.41 S	21.71 E	shrubland	434
Tshane Tshane (TSH), Botswana	24.17 S	21.89 E	wooded grassland	375
Vastrap Weapons Range (VST), South Africa	27.75 S	21.42 E	shrubland	270

3.2.2 Site selection and disturbance history

Only a small part of the Kalahari has been transformed by agriculture and human settlement (Scholes et al., 2002). The absence of standing water across the region is part of the reasons why it remains as one of the last places in Africa to be explored and settled (Skarpe, 1986). Following Scholes et al. (2002) sites were chosen to be representative of the surrounding area, with varying degrees of disturbance, none of which to the degree of being transformative. The only forms of disturbance include tree-cutting and grazing, with no history of cultivation. Accordingly, sites were selected to be

- Within a water limitation range between ca. 300-1000 mm of MAP.
- Representative of the surrounding landscape and vegetation.
- Away from from disturbance resulting from proximity to roads, water source, or cattle station.

Soils are deep, well drained eolian sand, except for Okwa River (22.4°), where sand is underlain by a hardpan at some meters. Rainfall is highly seasonal, with a dry season between May and September, coinciding with cooler temperatures.

3.2.3 Vegetation structure and pattern

The main determinant of vegetation composition and structure along the Kalahari sandsheet include rainfall, fire, herbivory, and nutrient availability (Scholes & Walker, 1993; Accatino et al., 2010). An interaction of these factors occurs across the transect, sometimes result in opposing trends in structure: as rainfall increases so does grass production, but also canopy cover and height, exerting a ceiling on peak grass biomass towards the middle of the gradient (Scholes et al., 2002). At the same time, fire frequency and intensity follows peak grass biomass, since the fuel of savanna fires is largely provided by dead grass biomass (Accatino et al., 2010), inhibiting the woody

component. The outcome is that the mixed life-form of trees and grasses occurs throughout the transect (Caylor et al., 2003).

3.2.4 Data collection

We used daily rainfall estimates between 2003-2016 from the Tropical Rainfall Measuring Mission (TRMM) (Huffman et al., 2007), available in the 3B42 product at 0.25° spatial resolution. Because of the highly seasonal nature of the Kalahari, quantification of annual precipitation was based on the hydrological year, starting on the first month ensuing the lowest mean monthly rainfall.

For a proxy measure of the ecosystem response to rainfall we used Moderate Resolution Imaging Spectroradiometer (MODIS) MOD13C1 (Terra) and MYD13C1 (Aqua), Enhanced Vegetation Index (EVI) across the same period (2003 - 2016), provided by the Land Processes Distributed Active Archive Center (LP DAAC) in 16 day, 0.05° resolution. Shuffling both Aqua and Terra satellite observations we arrived at 8 day observations, since the two satellites are staggered in time. Daily precipitation was summed over 8 day time periods to match the EVI time-series, and maximum EVI (EVI_{max}) was used to calculate the annual response for a given year. Ecosystem stability was estimated as $[\mu/\sigma]$, where μ is mean annual EVI_{max}, and σ is the standard deviation of annual EVI_{max} (Hallett et al., 2014).

3.2.5 Time-series and spectral analysis

We used wavelet analysis to decompose the EVI time-series to identify the relative contribution of each period to the overall EVI variability. Wavelets are well suited for analyzing non-stationary systems, who's periodic components change over time – a common aspect of ecological data (Cazelles et al., 2008). The wavelet power spectrum (WPS) provides information on the contribution of different frequencies to the overall signal. In other words, it provides information on the distribution of variance in the signal across different frequencies (f), and their localization over time (τ). Therefore, can help study transient effects.

We analyzed the frequency structure of the EVI time-series using functions implemented in the

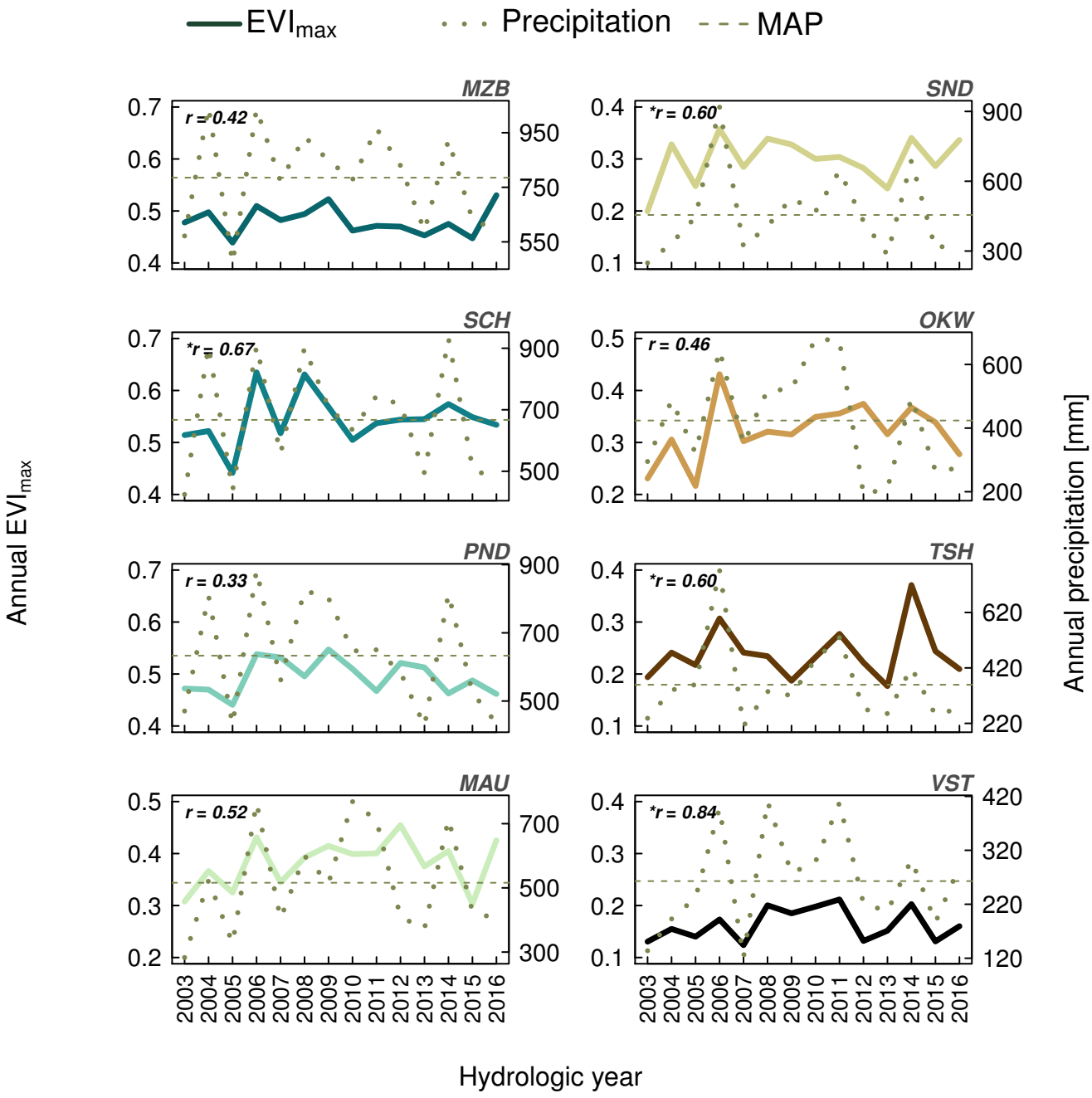

Figure 3.2: **Annual fluctuations in maximum Enhanced Vegetation Index (EVI_{max}), and TRMM-derived mean annual precipitation (MAP) between 2002-2016,** for 8 savanna sites ("MZB", "SCH", "PND", "MAU", "SND", "OKW", "TSH", "VST"), from the wettest, MZB (top-left), to the driest site, VST (bottom-right). "*" marks significant correlation at the 0.05 level.

R package WaveletComp (Roesch & Schmidbauer, 2014), following the methodology of Torrence & Compo (1998). To enable the interpretation of harmonic frequencies, non-linear trends in the EVI time-series were smoothed by local polynomial regression prior to spectral analysis. The smoothing parameter was chosen through trial and error as a multiple of 1/14 (corresponding to one year), to avoid interfering with seasonality, and then applied equally across all sites.

Statistical significance of wavelet power was assessed using bootstrap methods, testing the null hypothesis of “no periodicity", against a surrogate time-series representing a white noise process. The ridge of power within a band of periods was determined and used to help visualize which frequencies contribute the most at that time. A time-averaged WPS summarizes the overall power of the fundamental frequencies.

We explored the relationship between precipitation and vegetation response further by comparing the highest and lowest year observed. This included quantifying the positive vegetation response as the EVI anomaly [(maximum EVI_{max} - mean EVI_{max})/mean EVI_{max}] (Knapp & Smith, 2001), and plotted it against the positive precipitation anomaly. We compared this with the negative EVI anomaly [(mean EVI_{max} - minimum EVI_{max})/mean EVI_{max}], and its relationship with the negative precipitation anomaly. To allow for cross site comparisons we normalized by the mean. Also, since we are interested in comparisons of the potential response of the different savanna, knowing that the relationship with precipitation can be complex, we did not restrict the vegetation response to the corresponding precipitation anomaly year, and noted when otherwise.

3.3 Results

3.3.1 Variance components across time

We determined the WPS characterizing the response of different savanna across the regional gradient by using the wavelet approach. We found significant intra-seasonal response differences. Higher periodicity features, between periods 128 and 256 days, become increasingly important (explaining more of the variance of the series) going from “wet" to “dry" savanna (Fig. 3.3).

Ecosystem dynamics in the two wettest sites, MZB and SCH, was largely captured in the annual cycle, marked by a continuous ridge almost centered between periods 256 and 512 days, and little to no significant contribution from lower periods (intra-annual time-scales). In sharp contrast are the drier sites ($\leq$ 638 mm MAP) where transient but significant contribution to the total power (variance) occurred at the seasonal time-scale, periods coinciding with 128 through 256 days (shown here are PND at 638 mm and TSH at 375 mm, Fig. 3.3).

3.3.2 Ecosystem stability and extremes

Savanna closer to the drier end of the precipitation gradient, $<$ 600 mm, (MAU, OKW, SND, TSH and VST) had a much higher response range, $\pm$ 20% to 40% of the mean response (Fig. 3.4), in comparison with a more conservative response in “wetter" savanna, ranging between $\pm$ 5% to 12% of the mean. The symmetry of response (Fig. 3.4 and Figure A.1, Appendix) varied among sites, being symmetrical across the three wettest sites (MZB, SCH and PND), and the driest site (VST) where positive and negative response to rainfall variability were almost equal. On the other hand, savanna along the dynamic center of the transect (515 mm - 434 mm), including MAU, SND and OKW respectively, had an asymmetrical response, where the negative response to drought events was stronger than a positive response to the high annual precipitation. And finally, TSH, at 375 mm was the only site where a positive anomaly outweighed the negative response to annual precipitation. These response patterns translated to a broad range of stability across the transect. The three wettest savanna of the *woodland* had the highest stability (Fig. 3.5), with SCH the most stable, although its cv for annual rainfall was slightly higher than MZB and SCH, emphasizing a functional response to rainfall variability. In line with our wavelet analysis, savanna diverged in terms of stability along the 600 mm isopleth (Fig. 3.5), below which savanna remained within a close stability range. The overall response to precipitation extremes was highly contextual, rarely coinciding with precipitation minima and maxima. In only two out of the eight sites, MAU and OKW, did EVI minima coincide in time with precipitation minima (in 2003 for both sites), and in only one site, PND, was EVI maximum coincident with the year of maximum precipitation (in

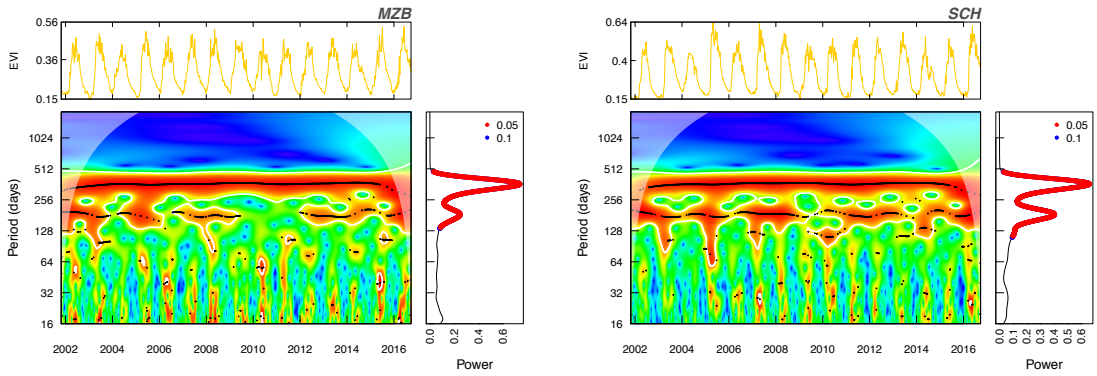

(a) Miombo woodland, MAP: 791 mm

(b) woodland, MAP: 671 mm

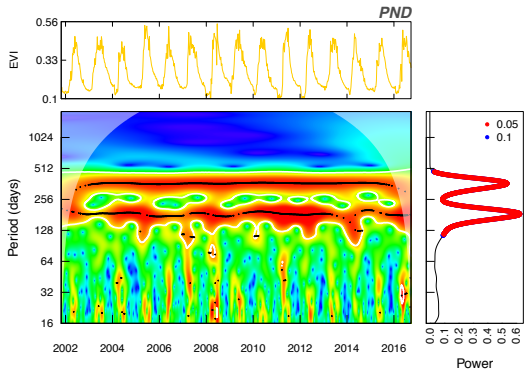

(c) woodland, MAP: 638 mm

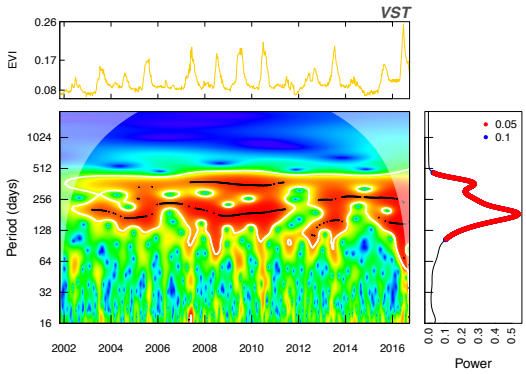

(d) shrubland, MAP: 270 mm

Figure 3.3: **Examples of ecosystem response patterns**, for four out of the eight savanna sites. From the wettest to the driest: *MZB, SCH, PND, TSH,* respectively. Showing (top) the time-series of MODIS EVI, and (below) the corresponding continuous wavelet power spectrum as a function of time and period, at 16-day temporal resolution. The colors code for power values, from low power (dark blue) to high (dark red). Black lines represent the ridge of wavelet power, while white contour lines indicate significant periodicity at the 5% significance level. Unreliable transform values due to boundary effects and scale are shaded, delineating the cone of influence.(right) Time-averaged power spectrum, indicating significance levels 10% (blue), and 5% (red).

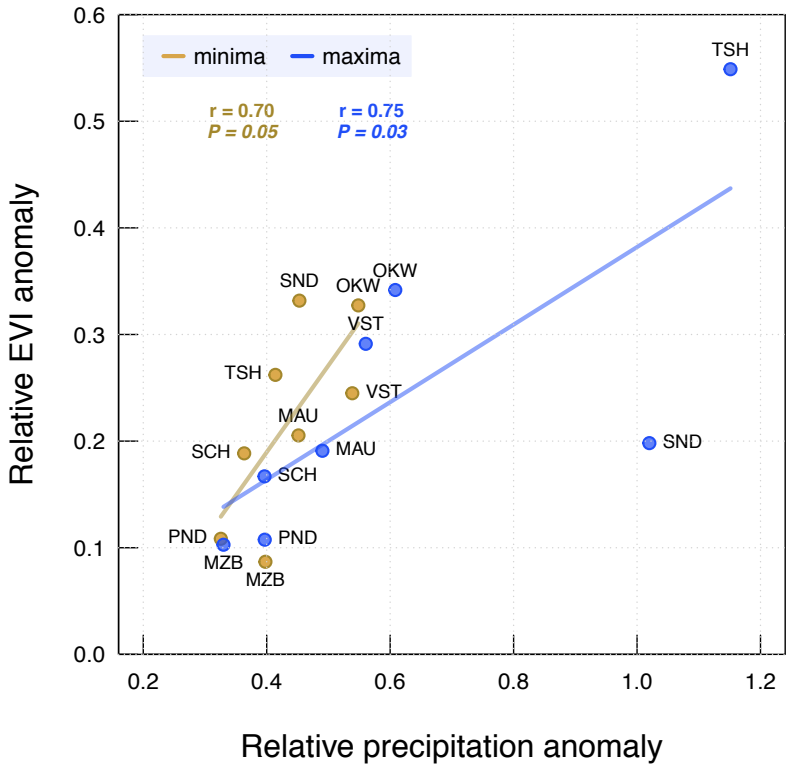

Figure 3.4: **Savanna response to extremes.** Relationship between precipitation anomaly and the relative vegetation response, EVI maxima and minima. The 2006 positive precipitation anomaly coincides with the response observed in SND and TSH (see Figure 3.1c).

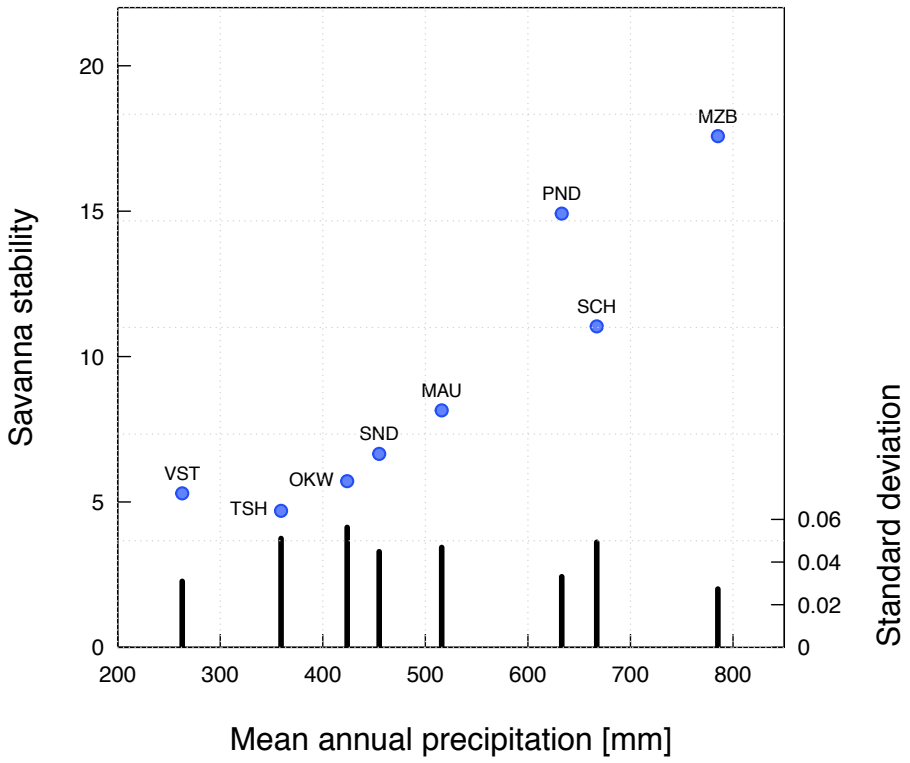

Figure 3.5: **Relationship between savanna stability [μ/σ] and mean annual precipitation (MAP)**, where μ is mean annual EVI_{max}, and σ is the standard deviation of annual EVI_{max}. Bars represent the standard deviation for EVI_{max}.

2006).

3.4 Discussion

Along a resource gradient and a highly seasonal rainfall pattern structurally variant savanna types responded differently to rainfall variability. In the wettest region of the transect, between 640 mm and 790 mm of MAP, *woodland* savanna exhibited the strongest buffer to interannual rainfall variability, supporting the framing of biotic control as a function of precipitation (Zhang et al., 2001; Huxman et al., 2005). This is demonstrated in a muted response to positive and negative rainfall anomalies observed in *woodland* savanna compared to *wooded grassland* and *shrubland* savanna. On the drier end, between 270 mm and 515 mm of MAP, EVI reflected environmental variability much more closely: a $\pm$40% relative precipitation anomaly resulted in a comparable response in EVI, between 20% to 40% of the mean.

Response patterns reflected different sensitivities to different time scales in a manner consistent with the relative contribution of trees and grasses. As savanna become more “woody" along a regional precipitation gradient, with greater contribution from trees and shrubs relative to grasses, their response became limited to the annual time-scale, with little to no sensitivity to fluctuations at the seasonal time-scale. This is in sharp contrast with the response we found of savanna in the drier region of the transect. Below ca. 600 mm lower periodicities (higher frequencies) become significant components of the response pattern. Relative growth rates of trees and grasses contribute to these differences in response patterns. If we consider that grasses represent the structural component of the system with the highest potential growth rates (Knapp & Smith, 2001), then our finding is closely in line with ground observations of the grass biomass (Scholes et al., 2002), showing a steady increase along the precipitation gradient, reaching a peak at ca. 600 mm, where it begins to decline under increased competition from woody plants (Scholes et al., 2002). The 600 mm isopleth marks the point along the transect where the EVI signal begins to show sensitivity to seasonal variability and a period of high variance between 4 to 8 months (Fig. 3.3). These different sensitivities among savanna types translated to differences in stability. As savanna become more

tree-dominated above 600 mm they also become less sensitive to seasonal patterns of resource availability, explaining the higher stability [μ/σ] among *woodland* savanna. An important distinction we wish to make here, is that despite the strength of our chosen stability measure owing to its simplicity and strict definition, we acknowledge limitations inherent in the fact that it is a ratio, therefore the possibility that larger differences in the mean among sites, relative to the standard deviation of the response, will influence differences in stability.

Alternatives to life history explanations justifying variable sensitivity to precipitation across resource gradients, also described as rainfall use efficiency (Huxman et al., 2004), include biogeochemical explanations. It is perceivable at the more mesic savanna, above 600 mm MAP, that water limitation becomes less important relative to other resources, such as soil nutrients and light, limiting the response capacity of the vegetation to precipitation, consistent with a transient maxima pattern (Seastedt & Knapp, 1993; Austin & Vitousek, 1998). While this might help explain the lower sensitivity of the *woodland* savanna, it does not on its own explain the major discrepancies we observed among the three *woodland* sites (Fig. 3.5), considering consistency in geomorphology and homogeneous soil conditions.

The symmetry of the response in the positive and the negative directions sheds light on the stability relationship with rainfall variability. A linear response to rainfall will result in a symmetrical response where wet and dry years have the same magnitude of effect on ecosystem response, while a saturating response to precipitation will result in an asymetrical response pattern, as decline outweighs growth (Gherardi & Sala, 2015). Across different biomes Knapp & Smith (2001) report a distinctly asymmetrical relationship between ecosystem productivity's relative maxima and relative minima, where the positive response is consistently higher, and sites converge along the 1:1 line (but some discrepancies are reported in Gherardi & Sala (2015)). We observed that the savanna on both extremes, very "wet", or very "dry", fall on, or very close to the line (Fig. 3.6), which suggests a linear response of EVI to precipitation. In contrast, the more dynamic savanna along the center of the transect had higher relative minima than maxima (S2, Supplement), indicating a saturating response to precipitation. We did not detect any significant lag effects at coarse

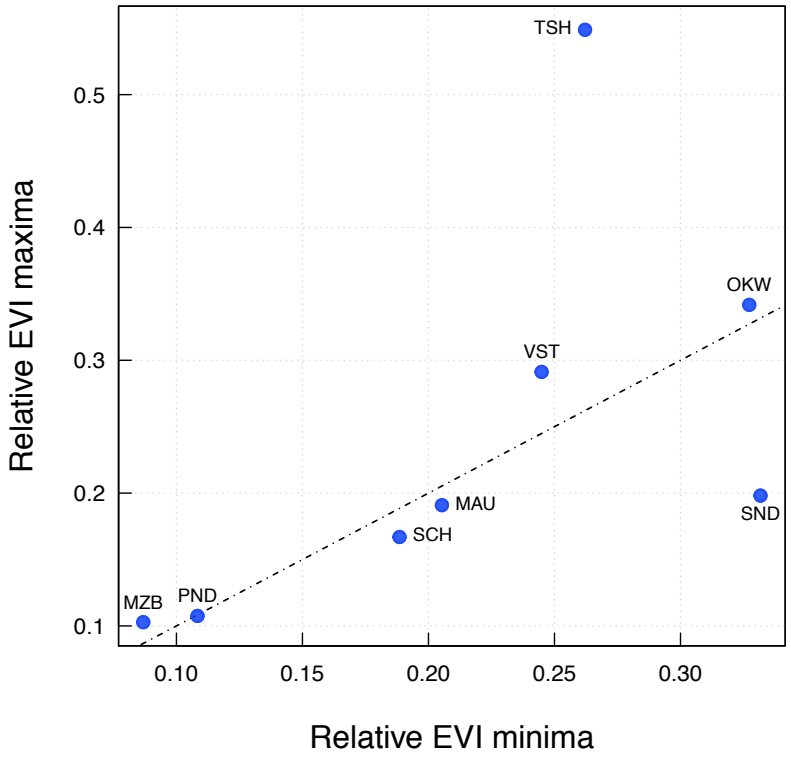

Figure 3.6: **Response symmetry.**

time-scales (i.e.: $>$ 1 year), nevertheless, previous year's precipitation might still have important effects. Out of the eight sites, only one had its peak response coincide with the wettest year, highlighting the importance of the previous year(s) and the contextual nature of vegetation response to extreme precipitation events.

3.5 Conclusion

Hypothetically, if rainfall variability had a direct effect on ecosystem response, then ecosystem dynamics becomes a reflection of the environment, and differences among ecosystems in their structure and composition would have little to no effect on their performance in the face of fluctuations. However, response patterns at different time-scales were different among savanna across a regional gradient and closely reflected the structure of savanna with respect to the co-dominance of trees and grasses. While we are not able to directly test mechanisms as might be possible in a controlled setting, the differences in response patterns across sites places them at different response capacities, which ultimately determines the degree to which savanna ecosystems can buffer change, rather than echo environmental fluctuation. Identifying when the coupling between structure and function results in variable sensitivities at different time scales can help identify where resource thresholds and ecosystem attributes are likely to result in their capacity to resist change. Observations from long term rainfall manipulation suggest that it does not always require a major degree of structural reordering to bring about a functional response (Knapp et al., 2012). We conclude that ecosystem structure separated savanna based on their sensitivity to environmental fluctuations, and this divergence occurred above 600 mm of MAP where grass biomass peaks and tree-dominated savanna begin (Huxman et al., 2005).

Chapter 4

Phase synchrony of savanna green-up and rainfall onset along a precipitation gradient

Abstract

The degree to which environmental variability is reflected in vegetation response can depend on the range of life history traits to cope with change. Savanna mark a unique biome defined by the coexistence of contrasting life histories: woody and gramineous plants with a range of different strategies for dealing with a seasonally arid and highly variable environment. We tested the degree to which different savanna communities across a rainfall gradient (270 mm - 791 mm, mean annual precipitation (MAP)) are coupled to rainfall onset by determining the synchrony between the day of year (DOY) when leaves first appear and rains start. While the time lag between green-up and rainfall decreased as we moved from wet to dry parts of the gradient, suggesting more arid savanna to be closely coupled with rainfall, tree-dominated savanna exhibited very clear phase synchrony which did not exist in the more arid sites. We discuss the implications of this synchrony as a stabilizing mechanism.

4.1 Introduction

Life history strategies distinguish tree and grass response patterns to meteorological cues. For savanna receiving below ca. 600 mm mean annual precipitation (MAP), grass primary productivity is linearly related to rainfall (Scholes et al., 2002). Above this point, competition from woody cover limits productivity (Scholes et al., 2002). Overall, the response of grasses is reflective of rainfall

variability, thereby grasses are responsible for the larger share of aggregate community variability as seen in satellite signals (Scanlon et al., 2002). The response of trees is less directly linked to rainfall in comparison (Borchert, 1994, 1999).

Phenological differences between trees and grasses become most apparent in relation to the onset of rainfall; the "on-off" switch in savanna (Scholes & Walker, 1993). Trees' capacity to tap into water and energy (carbohydrate) reserves allows for some buffer from abiotic forces, including such powerful cues as the onset of rainfall in arid ecosystems. The range of life history strategies used by tropical trees in response to a highly seasonal and variable environment can be seen in the prevalence of various functional types found within a single community (Borchert, 1999). Some trees show a tendency for flowering and shoot growth (flushing, or pre-rain green-up) preceding rainfall. This capacity is attributed to ecophysiological traits including wood density and stem water storage, and root access to subsoil water (Borchert, 1994). Meteorological cues, therefore, become insufficient in explaining community response patterns in tree-dominated savanna.

Here we consider differences among savanna in the degree to which ecosystem response mirrors rainfall variability and relate this to their composition, particularly the woody species component. We use satellite measurements of savanna vegetation response to daily rainfall and determine the degree to which season onset (green-up) relates to rainfall onset. The method of phase analysis allows for the determination of the degree of coupling between two oscillating signals by specifically measuring how two series fluctuate in the same direction, rising and falling with the same rhythm. The relevance of phase synchrony is highlighted in non-identical chaotic systems, with relevance to ecological communities (Blasius et al., 1999; Blasius & Stone, 2000). In such systems signal amplitudes are chaotic and uncorrelated. In other words, phase analysis allows access to more detailed synchrony information among signals which might otherwise prove uncorrelated as their maxima are not necessarily of the same magnitude. While different approaches can be used to decompose a signal into its phase and and time-dependent amplitude (Gabor, 1946; Yalçinkaya & Lai, 1997), interpretation can be challenging. We quantify phase synchrony based on a practical method appropriate for time series with distinct peaks or maxima. The basic approach relies on

identifiable or relevant maxima (or minima), and the fact that the time period between successive peaks (or troughs) in the signal corresponds to an increase in phase of 2π. Rather than maxima, for our purposes we extract phase based on the time period between green-up day of year (DOY), or in the case of the rainfall signal, it is the time period between rainfall onset DOY, whose synchrony we wish to determine across a 14-year record of satellite observations.

We hypothesize that savanna along a precipitation gradient will show different degrees of synchrony with rainfall. Specifically, we expect synchrony to reflect the dominance of the woody versus grass components in such a way that tree-dominated savanna will be less synchronized with rainfall as a result of their access to alternative sources of water, while savanna below 600 mm of MAP, will be closely coupled with rainfall (high synchrony), reflecting the importance of the grass component.

4.2 Methods

Relating two time series such as the abundance of two populations, or in our case, an ecosystem response to an environmental signal can employ different approaches. Traditionally this included measures of synchronization such as cross correlation statistics in the time domain, or coherence in the frequency domain, which depend on assumptions of linearity and stationarity. Qualities that are uncharacteristic of ecological signals, which can be non-stationary, short and irregular. A further shortfall with a correlation approach is the subtle but common case of irregular (nonidentical coupled) systems (Rosenblum et al., 1996; Pikovsky et al., 1997); where phases can be locked, oscillating simultaneously, but with independent magnitudes. This is also referred to as imperfect synchrony (Cazelles & Stone, 2003).

In keeping with the preference for simplicity and making the fewest assumptions we selected phase analysis to directly test the synchrony between savanna green-up and rainfall onset. To study phase synchronization of complex systems, it is important to develop a means of decomposing a signal into its phase and amplitude components. A general approach is to obtain the phase of a signal using the Hilbert transform (Gabor, 1946; Yalçinkaya & Lai, 1997). An alternative method

based on knowledge of the time intervals between spikes, or maxima is much easier to interpret (Blasius & Stone, 2000). Here we quantify the relationship between phases of savanna green-up date and rainfall onset date using a practical method to identify subtle patterns of synchronization (Blasius & Stone, 2000; Cazelles & Stone, 2003).

Temporally resolved data can be difficult to analyze because the data are autocorrelated thus violate the assumption of independence. To distinguish the observed Shannon-based synchrony metric as a true peak rather than an artifact of noise we test synchrony using amplitude-adjusted Fourier transform, a method of surrogate data which preserves the approximate Fourier spectrum (autocorrelation) while resampling values without replacement, thereby producing surrogates in which the original values are retained but rearranged in a way that largely preserves the spectrum and not the temporal information (Theiler et al., 1992; Schreiber & Schmitz, 2000).

4.2.1 Sites

The Kalahari Transect (KT) was chosen for its strong south to north rainfall gradient, across relatively homogeneous sandy soils and largely flat topography. Eight savanna sites were selected within a water-limited range between 270 mm - 791 mm of mean annual precipitation (MAP, Fig. 4.1). The southern most site marks the extent of the KT, at 27.75° S. The wettest site, at 16.75° S, still falls within a water-limitation range (Scanlon, 2003), with a distinct dry season spanning at least 6 months. The vegetation's floristic and structural attributes for the area between 10° S and 29° S are well documented by Scholes et al. (2002). Forming a progression of tree dominance, going from south to north, nutrient-rich, fine-leaved savanna give way to broad-leaves woodlands. To represent the structural types of savanna based on the dominance and diversity of woody species, we use data from Scholes et al. (2002) where a representative plot several ha in size was sampled at each site, between 1995 and 2000 (Fig. 4.3). The category "shrubs" defined as long-lived (>2 years) woody plants, and <2.5 m tall are included in the basal area, estimated using the T-square technique (Besag & Gleaves, 1973; Diggle, 1977) at 100 sample points at Maziba (0.5-1.5 m), and Sachinga (0-0.5 m). Tree basal area was estimated in 42 circular quadrats varying in radius

between 4-8 m depending on vegetation density, distributed over an area of 250 m by 300 m.

Following Scholes et al. (2002), sites were chosen to be representative of the surrounding area, with varying degrees of disturbance, none of which to the degree of being transformative. Soils are deep, well drained eolian sand, except for Okwa River (22.4°), where sand is underlain by a hardpan at some meters. Rainfall is highly seasonal, with a dry season between May and September, coinciding with cooler temperatures.

4.2.2 Data collection

For a proxy measure of the ecosystem response to rainfall we used Moderate Resolution Imaging Spectroradiometer (MODIS) MOD13C1 (Terra) and MYD13C1 (Aqua), Enhanced Vegetation Index (EVI), provided by the Land Processes Distributed Active Archive Center (LP DAAC) in 16 day, 0.05° resolution, between 2003 - 2016. Combining both Aqua and Terra satellite observations we arrived at 8 day observations since the EVI products are staggered in time. Daily EVI values were estimated using piecewise cubic Hermitean interpolation. We used daily rainfall estimates between 2003 - 2016 from the Tropical Rainfall Measuring Mission (TRMM) (Huffman et al., 2007), available in the 3B42 product at 0.25° spatial resolution. Because of the highly seasonal nature of the Kalahari, quantification of annual precipitation was based on the hydrological year, starting on the first month ensuing the lowest mean monthly rainfall. Daily precipitation was summed over 8 day time periods to match the EVI time-series, and maximum EVI (EVI_{max}) was used to calculate the annual response for a given year.

We used daily rainfall estimates from the Tropical Rainfall Measuring Mission (TRMM) (Huffman et al., 2007), available in the 3B42 product at 0.25° spatial resolution. Quantification of annual precipitation was based on the hydrological year, starting on the first month (August) ensuing the lowest mean monthly rainfall.

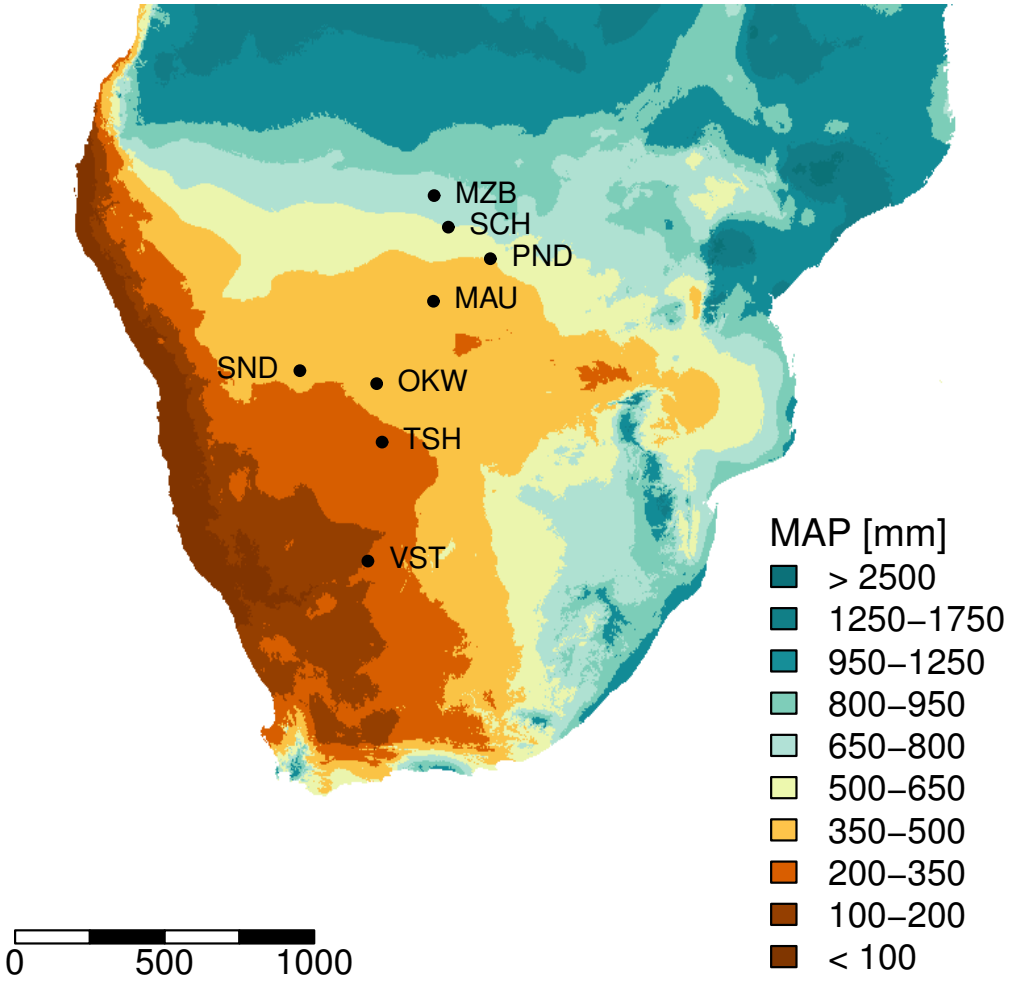

Figure 4.1: **Study sites across a regional precipitation gradient**, ∼1 km resolution [data from worldclim.org].

4.2.3 Determining green-up dates of growing season

As tree-grass composition changes along a gradient we are interested in the phenological attributes', specifically season onset or green-up, functional consequence on ecosystem response to rainfall variability. Different definitions have been applied to vegetation green-up in remote sensing studies, including the period of most rapid change in phenology, where a threshold approach makes sense. White et al. (1997) defined the green-up date as the day of year when NDVI rose above a 0.5 threshold of the maximum NDVI. Zhang et al. (2003) fitted a logistic function to each green-up cycle and defined green-up as when rates of maximum change in the derivative of the curve took place. Alternatively, here we define vegetation green-up as the moment when green leaves first appear in the landscape (Archibald & Scholes, 2007). This definition relaxes assumptions about growth rates. It also does not require *a priori* definition of minimum and maximum EVI. A particularly high degree of inter-annual variability, common to savanna ecology invalidates approaches which require a maximum and minimum value applicable across years (Archibald & Scholes, 2007).

We utilized the backward-looking moving average which utilizes a comparison of the EVI signal with a moving average to determine any departures from a trend, was first presented by Reed et al. (1994) to describe phenological phenomena across a wide range of land cover types in predominantly temperate climate, where an extended dormancy period is characteristic. The moving average time interval, originally 9 months, was modified for savanna (Archibald & Scholes, 2007) to account for a relatively short period when EVI drops to its minimum, for ca. two months. This is on account of many savanna tree species known to hold onto their leaves until late in the dry-season. Accordingly, tree green-up is determined as when the EVI signal is greater than the two-month moving average. For the KT we determined tree green-up as the first day past July 1 when the interpolated daily EVI value (piecewise cubic Hermitean interpolation) is greater than the average of the previous 7 time steps, or 56 days (ca. 2 months).

To explore the role of tree species composition with patterns of savanna green-up relative to rainfall onset we plotted basal area by woody species for each of the sites based on observations

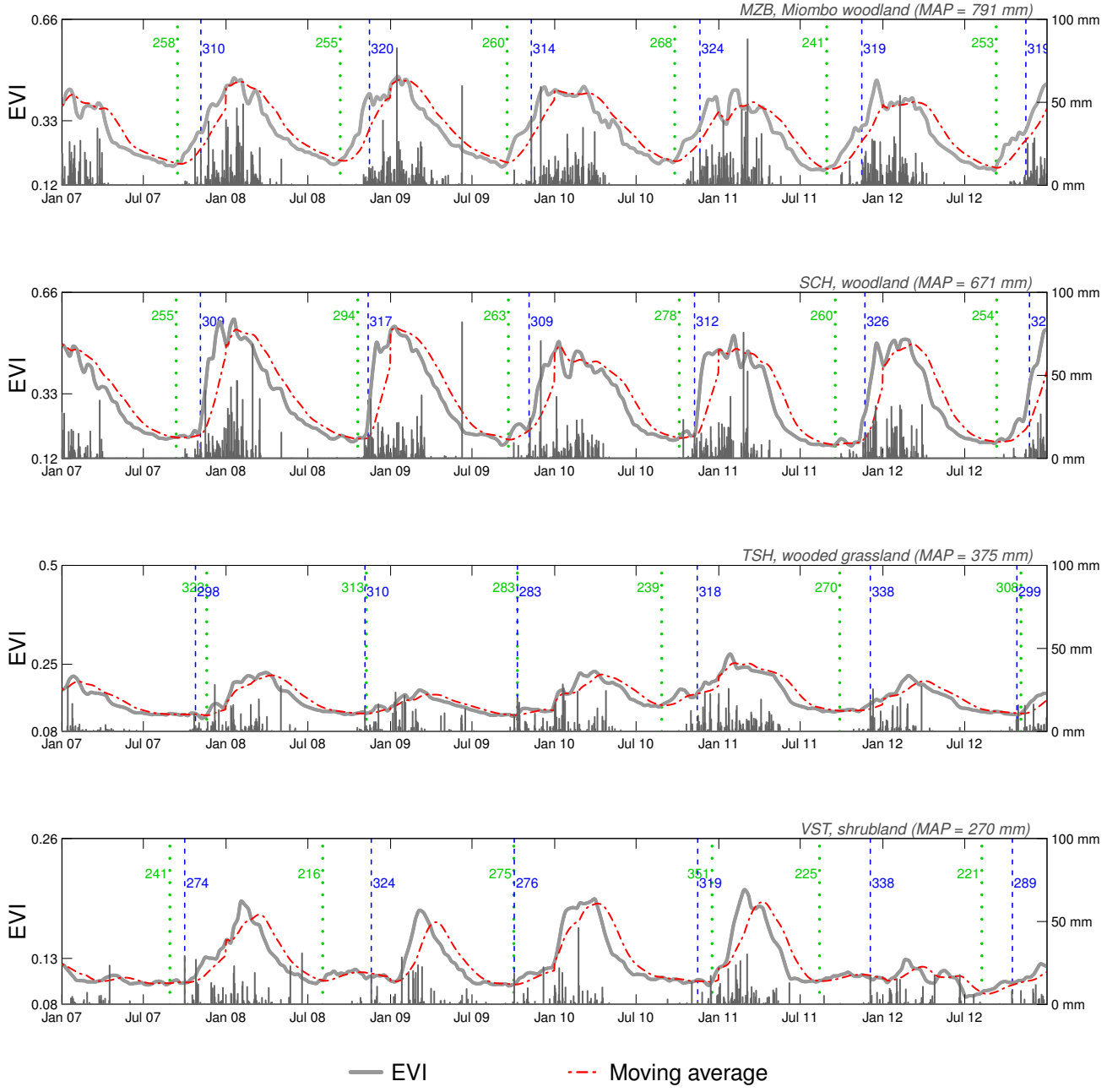

Figure 4.2: **Fifteen-year time series of MODIS EVI (solid grey line) and TRMM rainfall (vertical grey bars)** for the two wettest and two driest savanna, showing the method for determining green-up date. When the daily interpolated EVI time series crosses the 56-day moving average (ca. 2 months) green-up is marked (dotted vertical green lines). Rainfall onset (dashed vertical blue line) is based on a cumulative sum rainfall threshold of 5%. Day of year is shown for green-up and rainfall onset in green and blue, respectively.

made by Scholes et al. (2002) and hydrophenological observations for each species (Childes, 1988; Archibald & Scholes, 2007; Masia et al., 2018). We noted where species with known capacity for pre-rain green-up were in each site (Fig. 4.3).

4.2.4 Determining onset date of rainy season

Here we define the onset of the rainy season based on a climatological percentile to make comparisons across Southern Africa spanning a large gradient (270 mm to 971 mm, south to north). We determined rain onset as when the cumulative sum of daily rainfall reaches 5% of mean annual precipitation across the record for a given site (Guan et al., 2014). We chose a cumulative sum rainfall threshold of 5% to be more sensitive to small rainfall events, therefore more conservative than a larger threshold to better include grass response to rainfall, when compared to a 10% threshold.

4.2.5 Phase analysis and synchrony

One aspect of the degree to which different savanna are buffered from the environmental forcing we propose can be quantified as the degree of synchrony between pehnological attributes (green-up) and rainfall onset. We expect the woody-dominated savanna along the moist end of the gradient to be less dependent on rainfall relative to grasses, therefore less synchronized with rainfall than savanna < 600 mm of MAP.

Signal dependencies between ecosystem response and rainfall were determined through phase analysis. Traditional techniques such as correlation focusing on the signals themselves, influenced by irregularity of amplitudes, are likely to mask synchrony of two processes (Rosenblum et al., 2001; Cazelles & Stone, 2003). Also, while wavelet coherence in bivariate data analysis has been useful in describing temporal relationships specific to phase difference, one limitation with discrete wavelets is the need to designate period, which is specifically what we are testing to determine the degree of synchrony between green-up and rain-onset. Finally, interpretation of the phase difference in wavelet coherency analyses can be challenging.

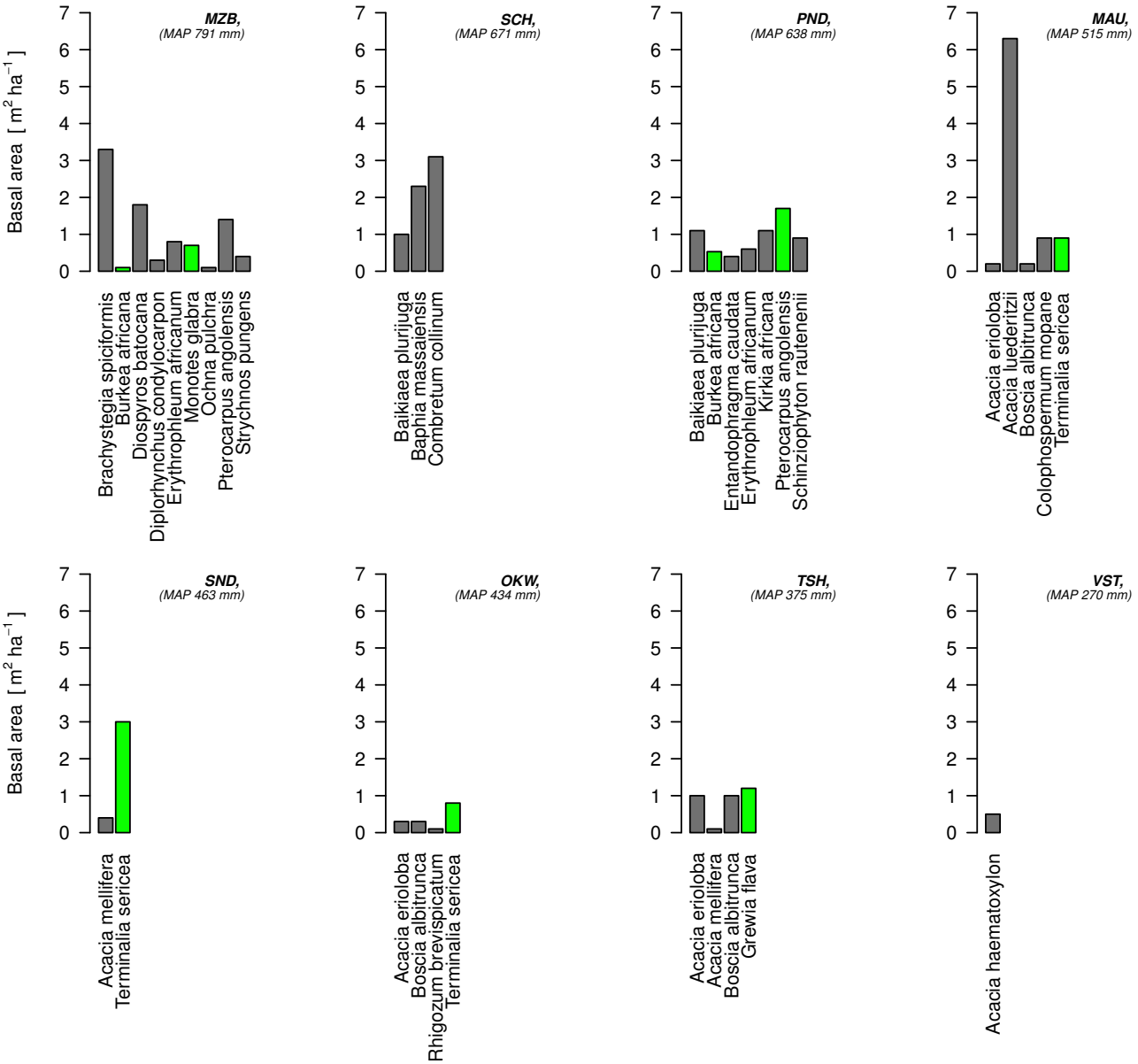

Figure 4.3: **Woody species composition making up 95% of basal area**, data from (Scholes et al., 2002). Green bars mark trees observed to exhibit pre-rain green-up (Childes, 1988; Archibald & Scholes, 2007; Masia et al., 2018).

We conducted a phase analysis using the Synchrony framework (Gouhier & Guichard, 2014) to detect the degree of synchrony between rainfall onset and green-up. This is done by:

1. Locating the local extrema of each time series (in our case, the green-up DOY and rainfall onset DOY mark the minima for the two signals).

2. Assigning them phase values (0 for the first extremum, 2π for the second extremum, 4π for the third, etc.).

3. Linearly interpolating between the extrema phase values yields phase values for points lying in between (Cazelles & Stone, 2003).

4. Computing instantaneous phase differences at each time step and plotting their distributions using fixed binning (equal number and size bins across the entire of possibilities, -π to π), determines the relationship between the two time series. Synchrony is high when a constant phase difference is preserved.

5. Calculating normalized entropy following Cazelles & Stone (2003) quantifies synchrony, by measuring how the two time-series move in the same direction, in corroboration with a statistical test of the null hypothesis, predicting no synchrony.

Details described below.

4.2.6 Estimating phase

In time series where maxima and minima can be readily determined, phase (ϕ) can be estimated assuming that the phase increase between any consecutive peaks is equal to 2π (Blasius et al., 1999). If t_n refers to the times when maxima (or minima) are reached, n = 1,2,3... , then values for the t_n phase are: $\phi(t_n) = 2\pi(n\text{-}1)$, which sets the first maxima to 0 phase. As a first approximation we assume the phase grows linearly with time, so that:

$$\phi(t) = 2\pi \left[\frac{(t - t_n)}{t_{n+1} - t_n} + (n - 1) \right] \tag{4.1}$$

The relationship between the two time series of phases can be determined by computing the frequency distribution of their instantaneous differences at each time step. Since we are interested in the mutual dependencies between season onset and rainfall onset we specifically chose green-up day of year (DOY) for the EVI time series, and rainfall onset DOY for the TRMM time series, as our minima.

4.2.7 Strength of synchrony

The frequency distribution of instantaneous phase differences for the green-up and rainfall onset time series provides information regarding the degree of synchronization (Tass et al., 1998; Rosenblum et al., 2001). Time series that are synchronized show a prominent peak in the distribution indicating a statistical tendency for the two series to be phase locked (Cazelles et al., 2014). A useful index of the strength of synchrony, how peaked the distribution is, employs the Shanon entropy:

$$S = \sum_{k=1}^{N_h} p_k \ln p_k, \tag{4.2}$$

where p_k is the proportion of points in the kth bin of the frequency histogram of phase differences and N_h is the number of bins. Accordingly, a Q_s index of normalized Shanon entropy is computed as follows (Cazelles et al., 2014):

$$Q_s = (\mathrm{S}_{\max} - S)/\mathrm{S}_{\max}, \tag{4.3}$$

where S is the Shannon entropy of the frequency histogram of phase differences, and $\mathrm{S}_{\max} = ln\ N_h$ is the maximum entropy possible (i.e, a uniform frequency distribution), such that Q_s falls between 0 for a uniform frequency distribution, and 1 for a dirac frequency distribution.

4.2.8 Testing phase synchronization using constrained realizations of phase randomization

It might not be obvious to distinguish a true peak in the distribution of phase difference from an artifact of noise, or of short time-series. A test of statistical significance is therefore needed to fairly evaluate phase synchrony. One approach is to compare the raw data's distribution to bootstrapped data by resampling the raw series using some randomized approach. A fair test preserves structures that are present in the data (Schreiber & Schmitz, 2000; Cazelles et al., 2014). Cazelles et al. (2014) demonstrate the inadequacy of the resampling series generated by white noise.

To test the null hypothesis stating that the observed synchrony is not different from what would be observed by chance, against the alternative, stating that the time series are synchronized we use a highly constrained surrogate data approach. The basic idea behind the method of Fourier component phase shuffling is to generate data with the same mean and autocorrelation, and thus the same power spectrum as the original data, because of the Wiener-Khinchin theorem, stating that the structure in the original time series is given by the autocorrelation function, or equivalently, by the Fourier power spectrum (Theiler & Prichard, 1996). A variant on the method is amplitude-adjusted Fourier transform (without replacement), which preserves all the properties of the original data, including the original values, while randomizing phase (Theiler et al., 1992; Schreiber & Schmitz, 2000).

The approach follows the following steps:

1. With exactly one green-up or rainfall onset date per year, we feed those dates into the surrogate procedure to get surrogate dates.

2. Those dates are used to make a surrogate series of periods with the same spectral characteristics as the original time series.

3. Next, we get the phases and phase differences and use those to calculate a surrogate Q_s value.

4. Comparison with 10,000 of these surrogate Q_s's determines significance.

4.3 Results

Onset of growing season (green-up) was different among savanna across the precipitation gradient relative to the onset of rainy season (Fig. 4.2). Pre-rain green-up occurred consistently across the 14 years of observation in three of the 8 sites: MZB, SCH, and SND (Appendix A.2). Among these three savanna sites green-up occurred between ca. 50 to 60 days prior to rainfall (Table 4.1). A less consistent timing of green-up relative to rainfall occurred for the *woodland* savanna PND and MAU, while a highly irregular pattern persisted across the 14-year record in the 3 driest savanna sites, OKW, TSH and VST, where green-up coincided with rainfall onset, preceded it, and in some years even succeeded rainfall (Appendix A.2). The shortest mean pre-rain green-up period occurred towards the drier end of the precipitation gradient, in the *wooded grassland* TSH, where green-up preceded rainfall by an average of 12 days. Similarly, in the driest site, *shrublad* VST, green-up averaged 23 days prior to rainfall. It also represented the most variable green-up DOY, averaging $\pm$48 days (Table 4.1).

Contrary to our expectation, synchrony between green-up and rainfall was highest overall in tree-dominated savanna, at the highest end of the precipitation gradient, with statistically significant phase synchrony observed in MZB and SCH (Q_s = 0.89 and 0.72, respectively, P-value < 0.05) (Table 4.1). Although green-up preceded rainfall every year in SND, we could not reject the null hypothesis that Q_s is not different from 0 (Q_s = 0.65, P-value = 0.8930). Savanna sites at drier part of the transect showed a uniform distribution of phase difference, with Q_s ranging between 0.01 and 0.57 (Fig. 4.4, Table 4.1). Consistent with this observation, the lowest phase synchrony, Q_s = 0.01 (P-value = 0.0128), coincided with the smallest difference between green-up DOY and rainfall onset, in the *wooded grassland* TSH (Table 4.1). Note that a positive value of phase difference is indicative of growing season preceding rainfall. Accordingly, for the 3 sites, MZB, SCH and SND where green-up is consistently prior to rainfall, all phase difference values are positive (Fig. 4.4).

Despite the higher likelihood for the presence of woody species with pre-rain green-up phenology as diversity increases up the precipitation gradient (Fig. 4.3), the presence of woody species

Table 4.1: **Phase synchrony of green-up and rainfall onset**, showing mean ± standard deviation of green-up and rainfall onset day of year (DOY), and their difference (rainfall onset - green-up) ± standard deviation. Three-letter abbreviations match the text and figures. Vegetation classification is based on (Scholes et al., 2002).

Site	Q_s	P-value	Green-up (DOY)	Rainfall (DOY)	Difference (days)	Vegetation type
Maziba (MZB) *Bay Forest* Zambia	**0.89**	0.0262	262 ±12	319 ±8	57 ±12	*Miombo*-woodland
Sachinga (SCH) *Agricultural Station* Namibia	**0.72**	0.0192	269 ±19	319 ±10	50 ±18	woodland
Pandamatenga (PND) *Agricultural Station* Botswana	0.93	0.0556	295 ±19	312 ±15	17 ±14	woodland
Maun (MAU) *Research Centre* Botswana	0.63	0.70	280 ±23	315 ±14	35 ±30	woodland
Sandveld (SND) *Research Station* Namibia	0.65	0.8930	247 ±15	311 ±17	64 ±20	wooded-grassland
Okwa (OKW) *River Crossing* Botswana	**0.57**	0.0160	267 ±28	308 ±15	41 ±25	shrubland
Tshane Tshane (TSH) Botswana	**0.01**	0.0128	287 ±22	299 ±22	12 ±30	wooded-grassland
Vastrap (VST) *Weapons Range* South Africa	0.32	0.1007	272 ±48	295 ±31	23 ±56	shrubland

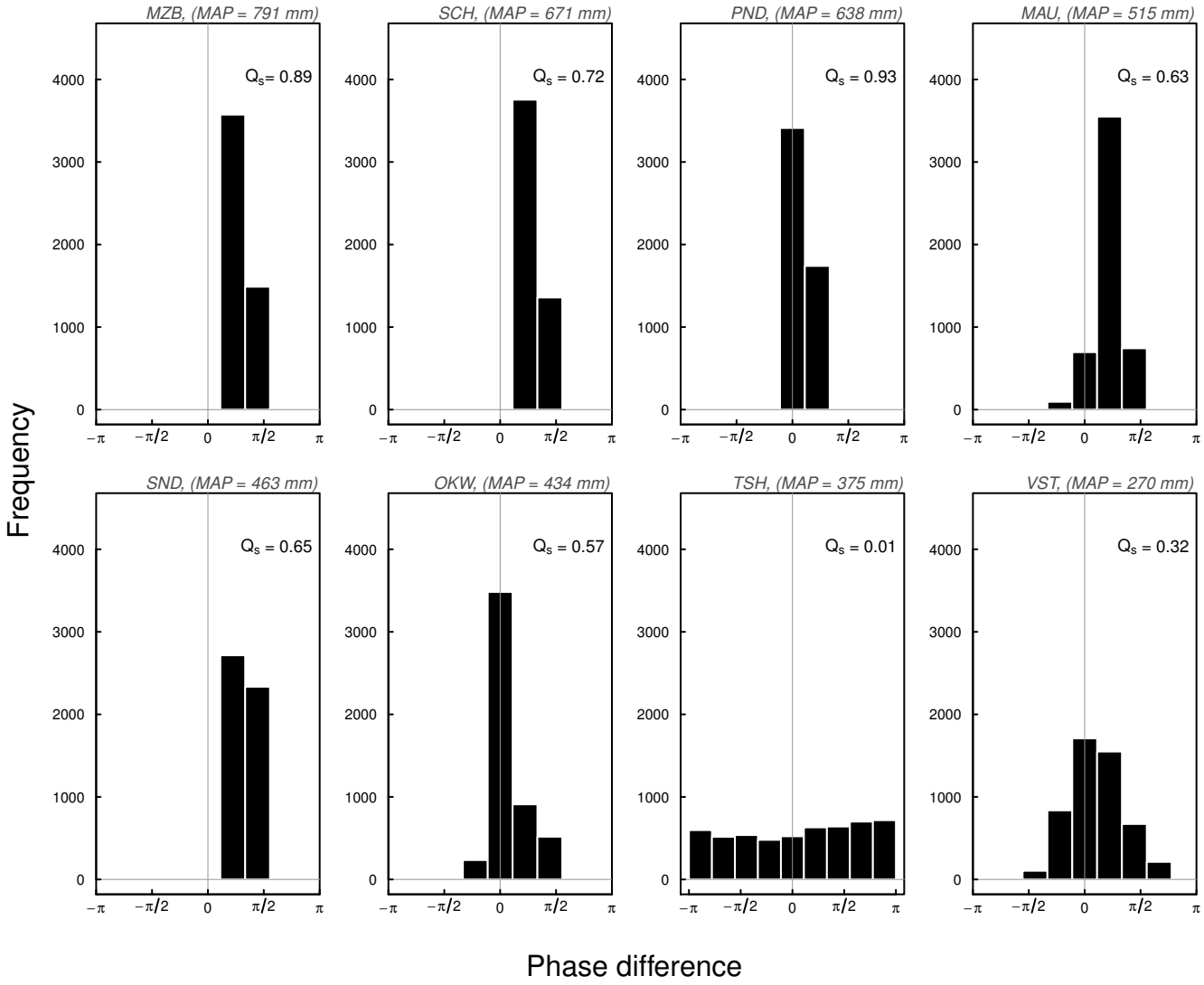

Figure 4.4: **Phase synchrony as detected by normalized Shanon entropy index,** Q_s, showing the frequency distribution of phase difference between green-up and rainfall onset in 8 savanna across a precipitation gradient. Scale shows the entire range of phase difference, -π to π (note π corresponds with approximately 6 months, and a positive value of phase difference means that green-up leads rainfall).

with pre-rain green-up phenology was indicated in all but two savanna, irrespective of MAP. Notable is the high dominance of *Terminalia sericea* in the *wooded grassland* SND; a tree known to flush early (Childes, 1988; Masia et al., 2018) (Fig. 4.3). SND is the only savanna site, below 600 mm MAP, with consistent pre-rain green-up across the observation record, however its phase synchrony (Q_s = 0.65) was found to be not different from 0 based on our constrained surrogate data approach. Although this synchrony is not statistically significant (P-value = 0.8930), consistent pre-rain phenology across 14 years of observation are in line with the dominance of textitTerminalia sericea driving the hydrophenology in this site.

4.4 Discussion

Our observations demonstrate a wider time lag between green-up and rainfall onset for savanna sites higher along a precipitation gradient, with greater woody species dominance (basal area) and diversity (Fig. 4.3). The woody basal area increases by 2.5 $m^2.ha^{-1}$ per 100 mm MAP (Scholes et al., 2002). In contrast with drier parts of the gradient where fewer woody species and a lower basal area (Table 4.1), show a shorter time lag between green-up and rainfall onset. This follows closely in line with similar observations across this region (Archibald & Scholes, 2007; Guan et al., 2014; Ryan et al., 2017). Surprisingly, however, the same savanna sites with the widest lag time between green-up and rainfall were highly synchronized with rainfall onset, such that green-up consistently preceded rainfall, and the two signals consistently tended towards phase locking. Here we consider a 14-year record to be a measure of consistency in aggregate community response. In contrast, the drier sites, which are more closely coupled with rainfall (short lag) were asynchronous with respect to the relationship between their leaf phenology and rainfall onset. The one exception is discussed next.

Phase synchrony coincided with pre-rain green-up, a trait largely driven by species composition. The exception we noted where pre-rain green-up occurred at 463 mm in the *wooded grassland* SND, consistently across a 14-year record, attributes this site's phenology to the dominance of tree species *Terminalia sericea* – known for pre-rain phenology. It also corroborates previous demon-

stration of the widespread occurrence of early green-up in this region (Ryan et al., 2017). While the increasing variability in rainfall onset moving down the gradient confounds our comparisons across sites, this exception to the general pattern across the transect supports the notion that pre-rain green-up phenology is largely a biotic process, expressed through community composition.

The pattern wherein tree-dominated savanna exhibit their leaves months prior to the onset of rainfall suggests a degree of buffer from the environment, attributable to the capacity which some tropical savanna tree species have to access stored water in their trunks (Borchert, 1994) or sub-surface (Do et al., 2008). This is in contrast to the more arid savanna where trees and grasses are more equally represented.

On the other hand, phase synchrony between green-up and rainfall was consistently high among tree-dominated savanna. Statistically significant, high phase synchrony occurred in the two wettest *woodland* sites, MZB and SCH (Q_s = 0.89 and 0.72, respectively, P-value $<$0.05), while little to no synchrony occurred among the more arid savanna, and only significant for the *shrubland*, OKW, and *wooded grassland*, TSH (Q_s = 0.57 and 0.01, respectively, P-value $<$0.05). This observation is exactly the opposite of our expectation.

At a first glance the observed synchrony seems counter intuitive with respect to our working framework, which predicts that any degree of buffering capacity within the vegetation community is in effect decoupling the vegetation response from environmental forcing. Perhaps the phase synchrony we observed can be better thought of with an intuitive example, or an analogy. Consider the pre-rain green-up as having a similar effect as winding a clock pendulum on every swing-cycle (growing-season). In the case of the savanna, accessing stored water is like the winding effect, ensuring on any given season an initial head-start, which can have some consequence in smoothing out variability in ecosystem response to variable rainfall.

Environmental cues for pre-rain green-up are not yet known, although different factors including photoperiod, day length and temperature show strong correlation with pre-rain phenology (Do et al., 2005; Archibald & Scholes, 2007). Photoperiod, or irradiance likely become more important in woodland savanna and the wetter parts of the transect, where light is more limiting. They are

also cues we expect to support the lower variability in vegetation phenology observed in the wetter parts of the transect. Further confounding our analysis is the fact that variability in rainfall onset was highest in the driest sites (Table 4.1).

Future research into the importance of plant water storage in dry tropical ecosystems, implementing different approaches, will help contextualize the significance of this coupling between ecosystem structure and function in water limited systems. For example, Borchert (1994) looked at the importance of water storage (plant and soil) at a regional scale. More recent work (Tian et al., 2018), employing satellite microwave radiometry as an index of plant and ground water storage (Ferrazzoli et al., 2002; Guglielmetti et al., 2007), evaluate the coupling between storage water and phenology globally. Finally, a limitation of our regional scale of inference includes the lack of ability to distinguish when early flushing trees drop their leaves and have to re-flush because of late rains. This understanding would help gauge the risks of pre-rain phenology and its importance in highly variable and seasonal ecosystems.

4.5 Conclusion

Along a precipitation gradient savanna varying in their structure, diversity and dominance of woody species demonstrate variable degrees of coupling with rainfall. Tree-dominated savanna at the wetter end of the gradient show a phenology with little to no sensitivity to rainfall onset, while more arid savanna sites, below 600 mm MAP, were closely coupled to rainfall in comparison. Concurrently, phase synchrony between green-up and rainfall onset showed the exact opposite pattern where tree-dominated savanna were synchronized with rainfall while sites with much lower basal area had a uniform, or flat distribution of phase synchrony.

Phase analysis of synchrony provides more detailed information about the synchrony relationship between two coupled oscillating signals. In addition to the time lag between two signals, information about the exact angle each signal is positioned at a given point in time allows further insight into more complex relationships, or as in our case, counter-intuitive results. In the case of early green-up we suggest that the resulting phase synchrony ends up having the effect of evening

out potential variability in ecosystem response from one year to the next. To put this in terms of plant water budget, access to storage water augments community productivity within a given year with a minimum amount of water every year, evening out inter-annual variability. Testing this "resetting effect" in different systems can help shed some light on the stabilizing mechanisms structurally diverse ecosystems have.

Chapter 5

Key Conclusions

At the outset I identified the common theme of this dissertation as how ecosystem structure determines response, or function. I examined this coupling at different scales: in an agroecosystem at the plot-level and among tropical savanna sites at the regional-level. The relevance of this coupling I explore in the context of restoring ecological function in agriculture by determining the role of diversity-driven process in two main main aspects of ecosystem function. First, in terms of complementary interactions, where interactions among different life-forms resulted in expanding agroecosystem water utilization. Similarly, I apply this coupling between ecosystem structure and function in exploring the role ecosystem composition plays in a regulatory capacity, by studying how different savanna ecosystems, varying in composition, respond in the face of rainfall variability. In all cases there was a strong coupling between ecosystem structure and function. As an example, the possible effects of incorporating a legume in a perennial grain intercrop, with contrasting ecosphysiology with respect to water acquisition and use, include a marked increase in productivity. Likely an outcome of expanding water utilization in the diversified agroecosystem, as indicated by stable isotope analysis. The conservative tone here is necessary caution, considering the novel nature of my results. Some of the key findings for these three studies are outlined here.

Co-occurring species can positively affect aggregate community response, redefining resource availability when alternative resource acquisition pathways are available to plant uptake and when species composition allows for the presence of complementary traits. In a novel perennial grain agroecosystem the intercropping of physiologically complementary species doubled aggregate community productivity. This level of overyielding was equivalent to the situation where nitro-

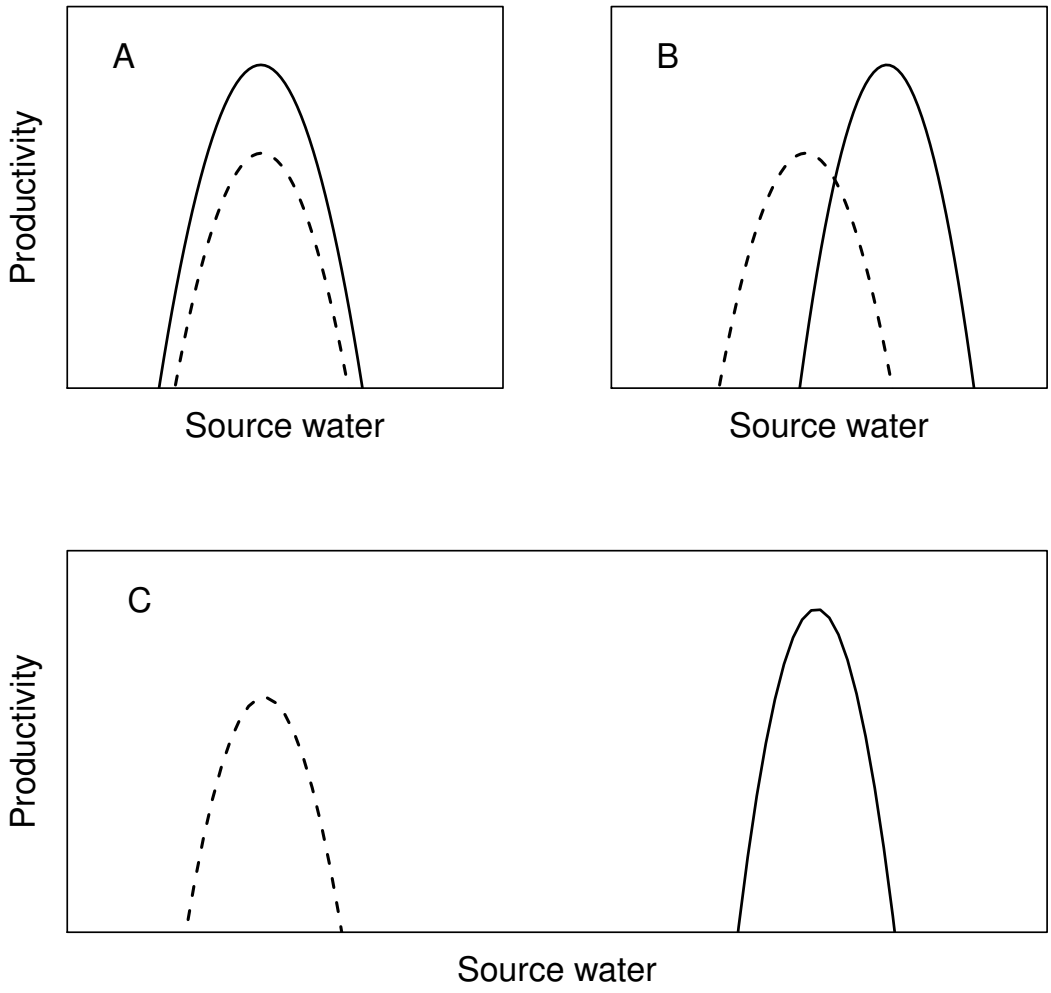

Figure 5.1: **Expanded conceptual framework for diversity-productivity relationships involving two species with varying degrees of overlap in niche space**. (A.) Null-hypothesis, no effect of species diversity on ecosystem productivity; (B.) Complementary resource use resulting in increased community productivity; (C.) A positive effect of complementary resource use involving an alternative water source.

gen (N) is not limiting plant growth. While a clear N-effect is observed in an N-addition trial, stable isotope analysis suggests that intercropping *Medicago sativa* accessed a water source unavailable to the perennial grain *Thinopyrum intermedium*, suggestive of resource partitioning in addition to the likely N-sparring effect. These results have direct implications for multipurpose, structurally diverse agroecosystems. They also suggest a reframing of how niche partitioning is envisioned to include the rare but important case of access to alternative sources of a resource, in our case, water.

Spectral analysis of savanna response to variable rainfall align with their sensitivity to anomalies. Savanna types responded differently to rainfall variability, closely tracking changes in the relative contribution of trees and grasses. Below 600 mm of mean annual precipitation savanna register both annual and seasonal fluctuation. Above the 600 mm isopleth woodland savanna are only responsive at the annual time scale. At opposite ends of the transect savanna sensitivity to wettest and driest years reveals large differences, where a $\pm$40% relative anomaly in precipitation resulted in a comparable response in EVI for savanna sites between 270 mm and 515 mm, compared to a 5% to 10% response for the wetter part of the transect, between 638 mm and 791 mm mean annual precipitation. The observation that precipitation extremes rarely coincided with the highest or lowest ecosystem response suggests a contextual response to rainfall events. An exciting direction for future work would be to explore the degree of carryover from different years across ecosystem types.

Contrasting life histories among savanna communities have bearing on the degree vegetation response mirrors environmental variability. While the time lag between savanna green-up and rainfall onset was more than double for some tree-dominated savanna relative to the drier savanna sites with progressively lower basal area, synchrony between green-up and rainfall onset showed the exact opposite pattern. Tree-dominated savanna showed a clear phase locking between the time when their first leaves appear and when the rains start. In contrast a more uniform

distribution of phase differences was characteristic of the driest sites, resulting in no significant synchrony to asynchrony between green-up and rainfall. Woody species composition, specifically the presence of tree species with a pre-rain phenology corroborates the hydrophenology expressed in the different savanna types. I suggest that the outcome of signal phase locking, where green-up leads rainfall onset can have a stabilizing effect in structurally diverse ecosystems, where access to storage water pre-sets the system on every season with a head-start.

5.0.1 Synthesis

An important distinction to make between the two scales of study, plot- and subcontinental-scale, relates to a trade-off between the ability to relate observations to process-level understanding, on the one hand, against facilitating generalizable inference of patterns and observations. To a larger degree, I am able to relate ecosystem structural attributes, and their effect on productivity, to differences in the acquisition and use of water, at the plot-level. However, it is not possible to determine the likelihood of encountering complementary effects in different communities, nor gain insight into when they tend to result in a change in ecosystem function in the absence of implementing these comparisons among different combinations of species assemblages, including a wide diversity of ecophysiologies, and across different conditions. In contrast, at the subcontinental-scale and across a gradient I am able to determine when and under which conditions savanna types respond differently to variable rainfall. However, at this scale of inference the number of interacting factors grows, challenging the possibility of isolating the underlying processes and mechanisms. In other words, the strength of this scale of inference lies in the ability to document when change occurs, rather than directly relate it to specific processes. Therefore, plot-level studies provide the process-level insight, while more spatially extensive studies provide the hierarchical framework.

Consequently, addressing the question of ecosystem structure and function at the broader scales has a lot to gain from plot-level insights. Nonetheless, additional confidence can be gained by approaching the problem from multiple perspectives while posing the question within the standing ecological framework. As an example, in chapters 2 and 3 I address the relationship between sa-

vanna composition to their regulatory capacity. Chapter 3 describes a clear pattern summarized in (Fig 3.4) of an increasingly muted ecosystem response, moving into higher tree-dominance at the wetter regions of the transect. Wavelet analysis confirms the higher sensitivity of drier savanna to the seasonal time scale relative to tree-dominated savanna (Fig. 3.3). While the phase analysis in chapter 4 confirms a muted response in tree-dominated savanna, with green-up occurring 50 to 60 days in advance of the rains (Table 4.1). Those same tree-dominated savanna showing a muted response surprisingly are also the most synchronized with rainfall. A counter-intuitive result, unless one considers the likely stabilizing effect of having a consistent head-start to the growing season through access to storage water. Another example of how the functional state of trees counteracts environmental influences. This pattern of stronger regulatory capacity in tree-dominated savanna fits directly within Zhang's ecohydrological framework associated with vegetation change (Zhang et al., 2001; Huxman et al., 2005).

References

Accatino, F., De Michele, C., Vezzoli, R., Donzelli, D., & Scholes, R. J. (2010). Tree-grass co-existence in savanna: Interactions of rain and fire. *Journal of Theoretical Biology*, 267(2), 235–242.

Adler, P. B. & Levine, J. M. (2007). Contrasting relationships between precipitation and species richness in space and time. *Oikos*, 116(2), 221–232.

Albertson, F. W. (1937). Ecology of mixed prairie in West Central Kansas. *Ecological Monographs*, 7(4), 481–547.

Archibald, S. & Scholes, R. J. (2007). Leaf green-up in a semi-arid African savanna: separating tree and grass responses to environmental cues. *Journal of Vegetation Science*, 18(4), 583.

Austin, A. T. & Vitousek, P. M. (1998). Nutrient dynamics on a precipitation gradient in Hawai'i. *Oecologia*, 113(4), 519–529.

Berkelhammer, M., Hu, J., Bailey, A., Noone, D. C., Still, C. J., Barnard, H., Gochis, D., Hsiao, G. S., Rahn, T., & Turnipseed, A. (2013). The nocturnal water cycle in an open-canopy forest. *Journal of Geophysical Research Atmospheres*, 118(17), 10225–10242.

Besag, J. & Gleaves, J. (1973). On the detection of spatial pattern in plant communities. *Bulletin of the International Statistical Institute*, 45, 153–158.

Blasius, B., Huppert, A., & Stone, L. (1999). Complex dynamics and phase synchronization in spatially extended ecological systems. *Nature*, 399(6734), 354–9.

Blasius, B. & Stone, L. (2000). Chaos ans phase synchronization in ecological systems. *International Journal of Bifurcation and Chaos*, 10(10)(10), 2361–2380.

Borchert, R. (1994). Soil and stem water storage determine phenology and distribution of tropical dry forest trees. *Ecology*, 75(5), 1437–1449.

Borchert, R. (1999). Climatic periodicity, phenology, and cambium activity in tropical dry forest trees. *IAWA Journal*, 20(3), 239–247.

Brand, W. A., Geilmann, H., Crosson, E. R., & Rella, C. W. (2009). Cavity ring-down spectroscopy ver-sus high-temperature conversion iso-tope ratio mass spectrometry; a casestudy ond2H andd18O of pure watersamples and alcohol/water mixtures. *Rapid Communications in Mass Spectrometry*, 23(12), 1879–1884.

Breshears, D. D., McDowell, N. G., Goddard, K. L., Dayem, K. E., Martens, S. N., Meyer, C. W., & Brown, K. M. (2008). Foliar absorption of intercepted rainfall improves woody plant water status most during drought. *Ecology*, 89(1), 41–47.

Brooks, J. R., Barnard, H. R., Coulombe, R., & McDonnell, J. J. (2010). Ecohydrologic separation of water between trees and streams in a Mediterranean climate. *Nature Geoscience*, 3(2), 100–104.

Bucini, G. & Hanan, N. P. (2007). A continental-scale analysis of tree cover in African savannas. *Global Ecology and Biogeography*, 16(5), 593–605.

Caylor, K., Shugart, H., Dowty, P., & Smith, T. (2003). Tree spacing along the Kalahari transect in southern Africa. *Journal of Arid Environments*, 54(2), 281–296.

Cazelles, B., Cazelles, K., & Chavez, M. (2014). Wavelet analysis in ecology and epidemiology: impact of statistical tests. *Journal of The Royal Society Interface*, 11(91), 20130585.

Cazelles, B., Chavez, M., Berteaux, D., Ménard, F., Vik, J. O., Jenouvrier, S., & Stenseth, N. C. (2008). Wavelet analysis of ecological time series. *Oecologia*, 156(2), 287–304.

Cazelles, B. & Stone, L. (2003). Detection of imperfect population synchrony in an uncertain world. *Journal of Animal Ecology*, 72(6), 953–968.

Chapin, F. S., Zavaleta, E. S., Eviner, V. T., Naylor, R. L., Vitousek, P. M., Reynolds, H. L., Hooper, D. U., Lavorel, S., Sala, O. E., Hobbie, S. E., Mack, M. C., & Díaz, S. (2000). Consequences of changing biodiversity. *Nature*, 405(6783), 234–42.

Childes, S. L. (1988). Phenology of nine common woody species in semi-arid, deciduous Kalahari Sand vegetation. *Vegetatio*, 79(3), 151–163.

Cleland, E. E., Collins, S. L., Dickson, T. L., Farrer, E. C., Gross, K. L., Gherardi, L. A., Hallett, L. M., Hobbs, R. J., Hsu, J. S., Turnbull, L., & Suding, K. N. (2013). Sensitivity of grassland plant community composition to spatial versus temporal variation in precipitation. *Ecology*, 94(8), 1687–1696.

Cox, T. S., Glover, J. D., Van Tassel, D. L., Cox, C. M., & DeHAAN, L. R. (2006). Prospects for Developing Perennial Grain Crops. *BioScience*, 56(8), 649–659.

Crews, T. E., Blesh, J., Culman, S. W., Hayes, R. C., Jensen, E. S., Mack, M. C., Peoples, M. B., & Schipanski, M. E. (2016). Going where no grains have gone before: From early to mid-succession. *Agriculture, Ecosystems and Environment*, 223, 223–238.

Dawson, T. E. (1998). Fog in the Californian redwood forest: ecosystem inputs and use by plants. *Oecologia*, 117, 476–485.

Dawson, T. E. & Ehleringer, J. R. (1991). Streamside trees that do not use stream water. *Nature*, 350, 335–337.

DePeters, E. (2012). Important attributes and changes on the horizon. In *California Alfafa and Grains Symposium* Davis, CA: UC Cooperative Extension.

Diggle, P. J. . (1977). The Detection of Random Heterogeneity in Plant Populations Author. *Biometrics*, 33(2), 390–394.

Do, F. C., Goudiaby, V. A., Gimenez, O., Diagne, A. L., Diouf, M., Rocheteau, A., & Akpo, L. E.

(2005). Environmental influence on canopy phenology in the dry tropics. *Forest Ecology and Management*, 215(1-3), 319–328.

Do, F. C., Rocheteau, A., Diagne, A. L., Goudiaby, V., Granier, A., & Lhomme, J. P. (2008). Stable annual pattern of water use by Acacia tortilis in Sahelian Africa. *Tree Physiology*, 28(1), 95–104.

Doak, D. F., Bigger, D., Harding, E. K., Marvier, M. A., O'Malley, R. E., Thomson, D., Oõmalley, R. E., & Thomson, D. (1998). The statistical inevitability of stability-diversity relationships in community ecology. *The American Naturalist*, 151(3), 264–276.

D'Odorico, P. & Bhattachan, A. (2012). Hydrologic variability in dryland regions: impacts on ecosystem dynamics and food security. *Philosophical Transactions of the Royal Society B: Biological Sciences*, 367(1606), 3145–3157.

Ehleringer, J. R. & Dawson, T. E. (1992). Water uptake by Plants: perspectives from stable isotope composition. *Plant, Cell and Environment*, 15, 1073–1082.

Ehleringer, J. R. & Osmond, C. B. (1989). Stable isotopes. In R. W. Pearcy, J. R. Ehleringer, H. A. Mooney, & P. W. Rundel (Eds.), *Plant phisiological ecology field methods and instrumentation* chapter Stable iso, (pp. 281–300). London: Chapman and Hall.

Ellsworth, P. Z. & Williams, D. G. (2007). Hydrogen isotope fractionation during water uptake by woody xerophytes. *Plant and Soil*, 291(1-2), 93–107.

Feng, X., Porporato, A., & Rodriguez-Iturbe, I. (2013). Changes in rainfall seasonality in the tropics. *Nature Climate Change*, 3(9), 811–815.

Ferrazzoli, P., Guerriero, L., & Wigneron, J. P. (2002). Simulating L-band emission of forests in view of future satellite applications. *IEEE Transactions on Geoscience and Remote Sensing*, 40(12), 2700–2708.

Gabor, D. (1946). Theory of communication. *Journal of the Institution of Electrical Engineers - Part I: General*, 93(26), 429–457.

Gherardi, L. A. & Sala, O. E. (2015). Enhanced precipitation variability decreases grass- and increases shrub-productivity. *Proceedings of the National Academy of Sciences*, 112(41), 12735–12740.

Good, S. P. & Caylor, K. K. (2011). Climatological determinants of woody cover in Africa. *Proceedings of the National Academy of Sciences*, 108(12), 4902–4907.

Gouhier, T. C. & Guichard, F. (2014). Synchrony: Quantifying variability in space and time. *Methods in Ecology and Evolution*, 5(6), 524–533.

Guan, K., Wood, E. F., Medvigy, D., Kimball, J., Pan, M., Caylor, K. K., Sheffield, J., Xu, X., & Jones, M. O. (2014). Terrestrial hydrological controls on land surface phenology of African savannas and woodlands. *Journal of Geophysical Research G: Biogeosciences*, 119(8), 1652–1669.

Guglielmetti, M., Schwank, M., Mätzler, C., Oberdörster, C., Vanderborght, J., & Flühler, H. (2007). Measured microwave radiative transfer properties of a deciduous forest canopy. *Remote Sensing of Environment*, 109(4), 523–532.

Hallett, L. M., Hsu, J. S., Cleland, E. E., Collins, S. L., Dickson, T. L., Farrer, E. C., Gherardi, L. A., Gross, K. L., Hobbs, R. J., Turnbull, L., & Suding, K. N. (2014). Biotic mechanisms of community stability shift along a precipitation gradient. *Ecology*, 95(6), 1693–1700.

Hector, A., Bell, T., Hautier, Y., Isbell, F., K??ry, M., Reich, P. B., van Ruijven, J., & Schmid, B. (2011). BUGS in the analysis of biodiversity experiments: Species richness and composition are of similar importance for grassland productivity. *PLoS ONE*, 6(3), 1–10.

Hector, A., Schmid, C., Beierkuhnlein, C., Caldeira, M. C., Diemer, M., Dimitrakopoulos, P. G., Finn, J. a., Freitas, H., Giller, P. S., Good, J., Harris, R., Hëgberg, P., Huss-danell, K., Joshi, J.,

Jumpponen, A., Körner, C., Leadley, P. W., Loreau, M., Minns, A., Mulder, C. P. H., O'donovan, G., Otway, S. J., Pereira, J. S., Prinz, A., Read, D. J., Scherer-lorenzen, M., Schulze, E. D., Siamantziouras, A.-S., Spehn, E. M., Terry, a. C., Troumbis, a. Y., Woodward, F. I., Yachi, S., & Lawton, J. H. (1999). Plant diversity and productivity experiments en European grasslands. *Science*, 286, 1123–1127.

Hervé-Fernández, P., Oyarzún, C., Brumbt, C., Huygens, D., Bodé, S., Verhoest, N. E., & Boeckx, P. (2016). Assessing the 'two water worlds' hypothesis and water sources for native and exotic evergreen species in south-central Chile. *Hydrological Processes*, 30(23), 4227–4241.

Hooper, D., Solan, M., Symstad, A., Diaz, S., Gessner, M. O., Buchmann, N., Degrange, V., Grime, P., Hulot, F., Mermillod-Blondin, F., Roy, J., Spehn, E., & van Peer, L. (2002). Species diversity , functional diversity and ecosystem functioning Species diversity , functional diversity , and ecosystem functioning. In M. Loreau, S. Naeem, & P. Inchausti (Eds.), *Biodiversity and ecosystem functioning: synthesis and perspectives.* chapter 17, (pp. 192–208). New York: Oxford University Press.

Hooper, D. U., Chapin III, F. S., Ewel, J. J., Hector, A., Inchausti, P., Lavorel, S., Lawton, J. H., Lodge, D. M., Loreau, M., Naeem, S., Schmid, B., Setälä, H., Symstad, A. J., Vandermeer, J., & Wardle, D. A. (2005). Effects of biodiversity on ecosystem functioning: a concensus of current knowledge. *Ecological Monographs*, 75(1), 3–35.

Horita, J. & Wesolowski, D. J. (1994). Liquid-vapor fractionation of oxygen and hydrogen isotopes of water from the freezing to the critical temperature. *Geochimica et Cosmochimica Acta*, 58(16), 3425–3437.

Hsu, J. S., Powell, J., & Adler, P. B. (2012). Sensitivity of mean annual primary production to precipitation. *Global Change Biology*, 18(7), 2246–2255.

Huffman, G. J., Bolvin, D. T., Nelkin, E. J., Wolff, D. B., Adler, R. F., Gu, G., Hong, Y., Bowman, K. P., & Stocker, E. F. (2007). The TRMM Multisatellite Precipitation Analysis (TMPA):

Quasi-Global, Multiyear, Combined-Sensor Precipitation Estimates at Fine Scales. *Journal of Hydrometeorology*, 8(1), 38–55.

Huxman, T. E., Smith, M. D., Fay, P. a., Knapp, A. K., Shaw, M. R., Loik, M. E., Smith, S. D., Tissue, D. T., Zak, J. C., Weltzin, J. F., Pockman, W. T., Sala, O. E., Haddad, B. M., Harte, J., Koch, G. W., Schwinning, S., Small, E. E., & Williams, D. G. (2004). Convergence across biomes to a common rain-use efficiency. *Nature*, 429(6992), 651–654.

Huxman, T. E., Wilcox, B. P., Breshears, D. D., Scott, R. L., Snyder, K. A., Small, E. E., Hultine, K., Pockman, W. T., & Jackson, R. B. (2005). Ecohydrological implications of woody plant encroachment. *Ecology*, 86(2), 308–319.

Knapp, A. K., Briggs, J. M., & Smith, M. D. (2012). Community stability does not preclude ecosystem sensitivity to chronic resource alteration. *Functional Ecology*, 26(6), 1231–1233.

Knapp, A. K. & Smith, M. D. (2001). Variation Among Biomes in Temporal Dynamics of Primary Aboveground Production. *Science*, 0(5), 481–484.

Lauenroth, W. K. & Sala, O. E. (1992). Long-term forage production of North American shortgrass steppe. *Ecological Applications*, 2(4), 397–403.

Liebman, M., Gibson, L. R., Sundberg, D. N., Heggenstaller, A. H., Westerman, P. R., Chase, C. A., Hartzler, R. G., Menalled, F. D., Davis, A. S., & Dixon, P. M. (2008). Agronomic and economic performance characteristics of conventional and low-external-input cropping systems in the central corn belt. *Agronomy Journal*, 100(3), 600–610.

Limm, E. B. & Dawson, T. E. (2010). Polystichum munitum (Dryopteridaceae) varies geographically in its capacity to absorb fog water by foliar uptake within the redwood forest ecosystem. *American Journal of Botany*, 97(7), 1121–1128.

Limm, E. B., Simonin, K. A., Bothman, A. G., & Dawson, T. E. (2009). Foliar water uptake: A

common water acquisition strategy for plants of the redwood forest. *Oecologia*, 161(3), 449–459.

Lin, G. & Sternberg, L. d. S. L. (1993). Hydrogen isotopic fractionation by plant roots during water uptake in coastal wetland plants. In *Stable isotopes and plant carbon-water relations* (pp. 497–510).

Lin, Y., Horita, J., & Abe, O. (2018). Adsorption isotope effects of water on mesoporous silica and alumina with implications for the land-vegetation-atmosphere system. *Geochimica et Cosmochimica Acta*, 223, 520–536.

Lloret, F., Lobo, A., Estevan, H., Maisongrande, P., Vayreda, J., & Terradas, J. (2007). Woody plant richness and NDVI response to drought events in Catalonian (northeastern Spain) forests. *Ecology*, 88(9), 2270–2279.

Masia, N. D., Stevens, N., & Archibald, S. (2018). Identifying phenological functional types in savanna trees. *African Journal of Range and Forage Science*, 35(2), 81–88.

Monteith, J. L. (1963). The water relations of plants. In A. J. Rutter & F. H. Whitehead (Eds.), *The water relations of plants* chapter Dew: facts, (pp. 37–56). Oxford: Blackwells.

National Research Council (2001). *Grand Challenges in environmental sciences*. Washington DC: National Academies Press.

Nippert, J. B. & Knapp, A. K. (2007). Linking water uptake with rooting patterns in grassland species. *Oecologia*, 153(2), 261–272.

Nippert, J. B., Wieme, R. A., Ocheltree, T. W., & Craine, J. M. (2012). Root characteristics of C 4 grasses limit reliance on deep soil water in tallgrass prairie. *Plant and Soil*, 355(1-2), 385–394.

Noy-Meir, I. (1973). Desert Ecosystems: Environment and Producers. *Annual Review of Ecology and Systematics*, 4(1), 25–51.

O'Brien, E. M. (1993). Climatic Gradients in Woody Plant Species Richness: Towards an Explanation Based on an Analysis of Southern Africa's Woody Flora. *Journal of Biogeography*.

Pikovsky, A. S., Rosenblum, M. G., Osipov, G. V., & Kurths, J. (1997). Phase synchronization of chaotic oscillators by external driving. *Physica D: Nonlinear Phenomena*, 104, 219–238.

Ratzmann, G., Gangkofner, U., Tietjen, B., & Fensholt, R. (2016). Dryland Vegetation Functional Response to Altered Rainfall Amounts and Variability Derived from Satellite Time Series Data. *Remote Sensing*, 8(12), 1026.

Reed, B. C., Brown, J. F., VanderZee, D., Loveland, T. R., Merchant, J. W., & Ohlen, D. O. (1994). Measuring phenological variability from satellite imagery. *Journal of Vegetation Science*, 5(5), 703–714.

Roesch, A. & Schmidbauer, H. (2014). WaveletComp: computational wavelet analysis. http://www.hs-stat.com/projects/WaveletComp/WaveletComp_guided_tour.pdf/.

Rosenblum, M., Pikovsky, A., & Kurths, J. (2001). Phase synchronization: from theory to data analysis. *Handbook of biological ...*.

Rosenblum, M. G., Pikovsky, a. S., & Kurths, J. (1996). Phase synchronization of chaotic oscillators. *Physical Review Letters*, 76(11), 1804–1807.

Ryan, C. M., Williams, M., Grace, J., Woollen, E., & Lehmann, C. E. (2017). Pre-rain green-up is ubiquitous across southern tropical Africa: implications for temporal niche separation and model representation. *New Phytologist*, 213(2), 625–633.

Sankaran, M., Hanan, N. P., Scholes, R. J., Ratnam, J., Augustine, D. J., Cade, B. S., Gignoux, J., Higgins, S. I., Le Roux, X., Ludwig, F., Ardo, J., Banyikwa, F., Bronn, A., Bucini, G., Caylor, K. K., Coughenour, M. B., Diouf, A., Ekaya, W., Feral, C. J., February, E. C., Frost, P. G. H., Hiernaux, P., Hrabar, H., Metzger, K. L., Prins, H. H. T., Ringrose, S., Sea, W., Tews, J.,

Worden, J., & Zambatis, N. (2005). Determinants of woody cover in African savannas. *Nature*, 438(7069), 846–849.

Scanlon, T. M. (2003). Inferred controls on tree/grass composition in a savanna ecosystem: Combining 16-year normalized difference vegetation index data with a dynamic soil moisture model. *Water Resources Research*, 39(8), 1–13.

Scanlon, T. M., Albertson, J. D., Caylor, K. K., & Williams, C. A. (2002). Determining land surface fractional cover from NDVI and rainfall time series for a savanna ecosystem. *Remote Sensing of Environment*, 82(2-3), 376–388.

Scanlon, T. M., Caylor, K. K., Manfreda, S., Levin, S. A., & Rodriguez-Iturbe, I. (2005). Dynamic response of grass cover to rainfall variability: Implications for the function and persistence of savanna ecosystems. *Advances in Water Resources*, 28(3), 291–302.

Scholes, R. (2016). Ecology for a small planet. In *Inaugural Speech* Johannesburg, South Africa: WITS University.

Scholes, R. J., Dowty, P. R., Caylor, K., Parsons, D. a. B., Frost, P. G. H., & Shugart, H. H. (2002). Trends in savanna structure and composition along an aridity gradient in the Kalahari. *Journal of Vegetation Science*, 13(3), 419–428.

Scholes, R. J. & Walker, B. B. H. (1993). *An African Savanna: Synthesis of the Nylsvley Study*. Cambridge: Cambridge University Press.

Schönherr, J. & Schmidt, H. (1979). water permeability by plant cuticles: dependence of permeability coeficients of cuticular transpiration on vapor presssure saturation deficit. *Planta*, 144, 391–400.

Schreiber, T. & Schmitz, A. (2000). Surrogate time series. *Physica D: Nonlinear Phenomena*, 142(3-4), 346–382.

Seastedt, T. R. & Knapp, A. K. (1993). Consequences of Nonequilibrium Resource Availability Across Multiple Time Scales: The Transient Maxima Hypothesis. *The American Naturalist*, 141(4), 621–633.

Skarpe, C. (1986). Plant community structure in relation to grazing and environmental changes along a north-south transect in the western Kalahari. *Vegetatio*, 68(1), 3–18.

Slatyer, R. (1958). *Availability of water to plants*. Technical report, UNESCO Arid Zone Research XI.

Sprenger, M., Leistert, H., Gimbel, K., & Weiler, M. (2016). Illuminating hydrological processes at the soil-vegetation-atmosphere interface with water stable isotopes. *Reviews of Geophysics*, 54(3), 674–704.

Stock, B. & Semmens, B. (2016a). MixSIAR GUI User Manuel. Version 3.1. https://github.com/brianstock/MixSIAR/ (Accessed. 21 September, 2018 Web).

Stock, B. C. & Semmens, B. X. (2016b). Unifying error strucctures in commonly used biotracer mixing models. *Ecology*, 97(3), 576–582.

Sun, G., Coffin, D. P., & Lauenroth, W. K. (1997). Comparison of root distributions of species in North American grasslands using GIS. *Journal of Vegetation Science*, 8(4), 587–596.

Tass, P., Rosenblum, M., Weule, J., Kurths, J., Pikovsky, A., Volkmann, J., Schnitzler, A., & Freund, H.-J. (1998). Detection of n:m phase locking from noisy data: application to magnetoencephalography. *Physical Review Letters*, 81(15), 3291.

Theiler, J., Eubank, S., Longtin, A., Galdrikian, B., & Doyne Farmer, J. (1992). Testing for nonlinearity in time series: the method of surrogate data. *Physica D: Nonlinear Phenomena*, 58(1-4), 77–94.

Theiler, J. & Prichard, D. (1996). Constrained-realization Monte-Carlo method for hypothesis testing. *Physica D: Nonlinear Phenomena*, 94(4), 221–235.

Thorburn, P. J. & Mensforth, L. J. (1993). Sampling water from alfalfa (Medicago sativa) for analysis of stable isotopes of water. *Communications in Soil Science and Plant Analysis*, 24(5-6), 549–557.

Tian, F., Wigneron, J. P., Ciais, P., Chave, J., Ogée, J., Peñuelas, J., Ræbild, A., Domec, J. C., Tong, X., Brandt, M., Mialon, A., Rodriguez-Fernandez, N., Tagesson, T., Al-Yaari, A., Kerr, Y., Chen, C., Myneni, R. B., Zhang, W., Ardö, J., & Fensholt, R. (2018). Coupling of ecosystem-scale plant water storage and leaf phenology observed by satellite. *Nature Ecology and Evolution*, 2(9), 1428–1435.

Tilman, D., Wedin, D., & Knops, J. (1996). Productivity and sustainability influenced by biodiversity in grassland ecosystems. *Nature*, 379(6567), 718–720.

Torrence, C. & Compo, G. P. (1998). A practical guide to wavelet analysis. *Bull. Am. Meteor. Soc.*, 79(1), 61–78.

Walker, B. (2001). Tropical Savanna. In F. S. Chapin III, O. E. Sala, & E. Huber-Sannwald (Eds.), *Global biodiversity in a changing environment: scenarios for the 21 st century* (pp. 139–156). New York: Springer.

Weaver, J. (1966). *Prairie plants and their environment: a fifty year study from the midwest*. Lincoln: University of Nebraska Press.

Welp, L. R., Lee, X., Kim, K., Griffis, T. J., Billmark, K. A., & Baker, J. M. (2008). ??18O of water vapour, evapotranspiration and the sites of leaf water evaporation in a soybean canopy. *Plant, Cell and Environment*, 31(9), 1214–1228.

Weltzin, J. F., Loik, M. E., Schwinning, S., Williams, D. G., Fay, P. a., Haddad, B. M., Harte, J., Huxman, T. E., Knapp, A. K., Lin, G., Pockman, W. T., Shaw, M. R., Small, E. E., Smith, M. D., Smith, S. D., Tissue, D. T., & Zak, J. C. (2003). Assessing the Response of Terrestrial Ecosystems to Potential Changes in Precipitation. *BioScience*, 53(10), 941.

West, A. G., Goldsmith, G. R., Brooks, P. D., & Dawson, T. E. (2010). Discrepancies between isotope ratio infrared spectroscopy and isotope ratio mass spectrometry for the stable isotope analysis of plant and soil waters. *Rapid Communications in Mass Spectrometry*, 24(14), 1948–1954.

White, M. A., Thornton, P. E., & Running, S. W. (1997). A continental phenology model for monitoring vegetation responses to interannual climatic variability. *Global Biogeochemical Cycles*, 11(2), 217–234.

Williams, C. A. & Albertson, J. D. (2005). Contrasting short- and long-timescale effects of vegetation dynamics on water and carbon fluxes in water-limited ecosystems. *Water Resources Research*, 41(6), 1–13.

Wojdak, J. M. & Mittelbach, G. G. (2007). Consequences of niche overlap for ecosystem functioning: An experimental test with pond grazers. *Ecology*, 88(8), 2072–2083.

Woodward, F. I. & Lomas, M. R. (2004). Simulating vegetation processes along the Kalahari transect. *Global Change Biology*, 10(3), 383–392.

Yalçinkaya, T. & Lai, Y. C. (1997). Phase characterization of chaos. *Physical Review Letters*, 79(20), 3885–3888.

Zhang, B., Li, F. M., Huang, G., Cheng, Z. Y., & Zhang, Y. (2006). Yield performance of spring wheat improved by regulated deficit irrigation in an arid area. *Agricultural Water Management*, 79(1), 28–42.

Zhang, L., Dawes, W. R., & Walker, G. R. (2001). Response of Mean Annual Evapotranspiration to Vegetation changes at Catchment Scale. *Water Resources*, 37(3), 701–708.

Zhang, X., Friedl, M. A., Schaaf, C. B., Strahler, A. H., Hodges, J. C. F., Gao, F., Reed, B. C., & Huete, A. (2003). Monitoring vegetation phenology using MODIS. *Remote Sensing of Environment*, 84(3), 471–475.

Appendix A

Appendix

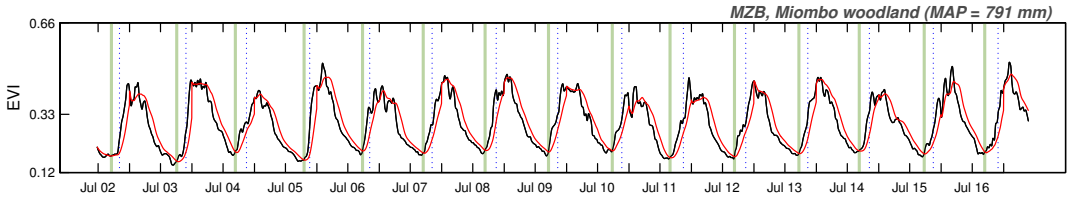
MZB, Miombo woodland (MAP = 791 mm)
EVI
0.66
0.33
0.12
Jul 02
Jul 03
Jul 04
Jul 05
Jul 06
Jul 07
Jul 08
Jul 09
Jul 10
Jul 11
Jul 12
Jul 13
Jul 14
Jul 15
Jul 16

(a)

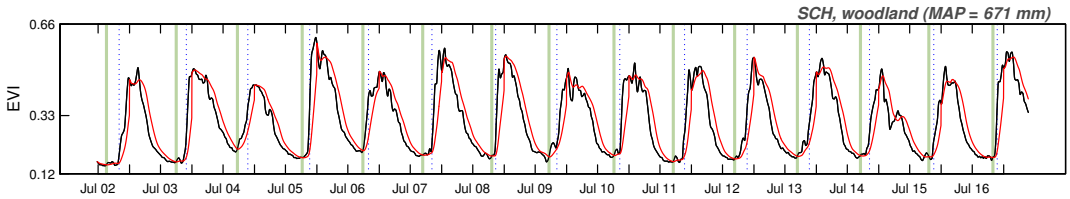
SCH, woodland (MAP = 671 mm)
EVI
0.66
0.33
0.12
Jul 02
Jul 03
Jul 04
Jul 05
Jul 06
Jul 07
Jul 08
Jul 09
Jul 10
Jul 11
Jul 12
Jul 13
Jul 14
Jul 15
Jul 16

(b)

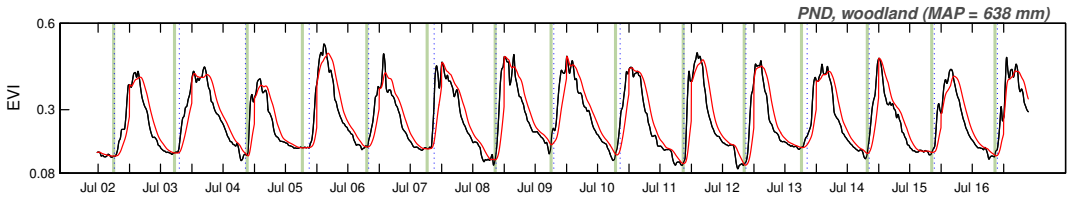
PND, woodland (MAP = 638 mm)
EVI
0.6
0.3
0.08
Jul 02
Jul 03
Jul 04
Jul 05
Jul 06
Jul 07
Jul 08
Jul 09
Jul 10
Jul 11
Jul 12
Jul 13
Jul 14
Jul 15
Jul 16

(c)

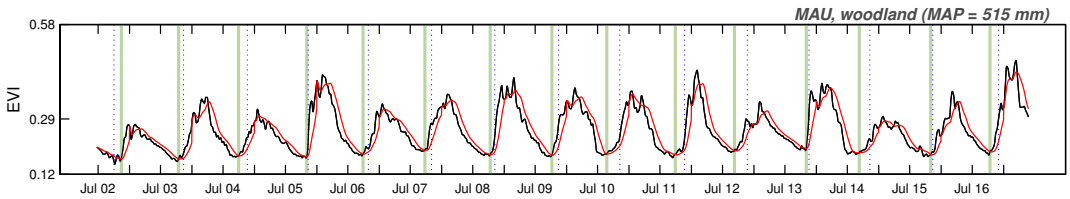
MAU, woodland (MAP = 515 mm)
EVI
0.58
0.29
0.12
Jul 02
Jul 03
Jul 04
Jul 05
Jul 06
Jul 07
Jul 08
Jul 09
Jul 10
Jul 11
Jul 12
Jul 13
Jul 14
Jul 15
Jul 16

(d)

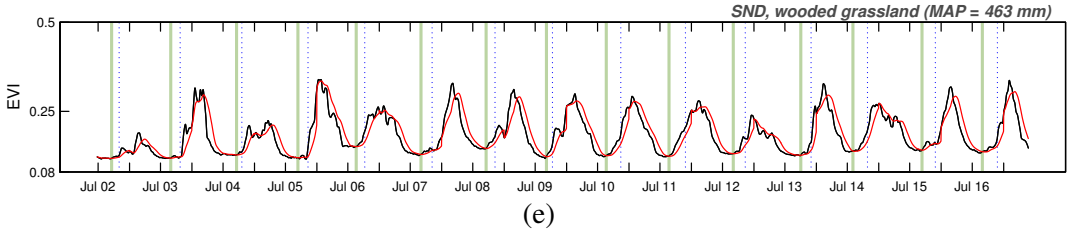

(e)

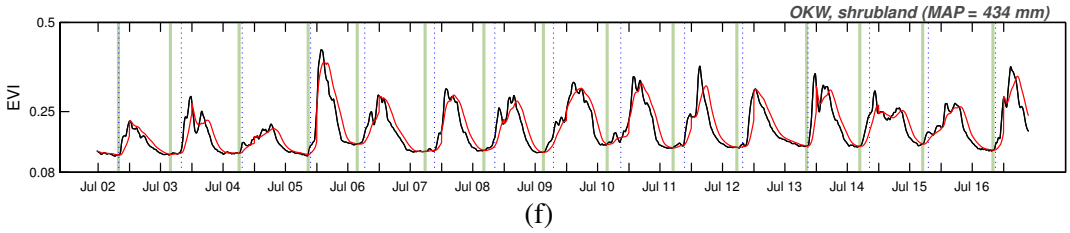

(f)

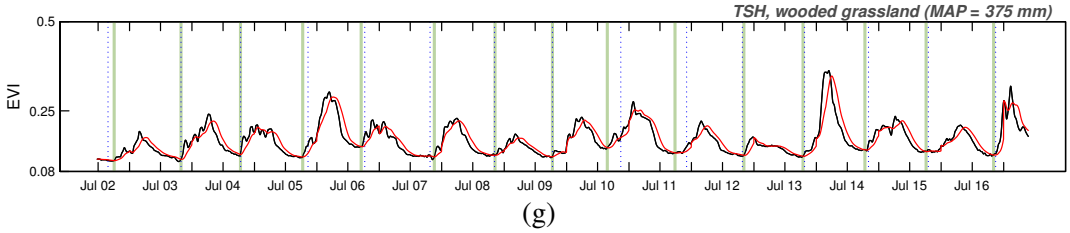

(g)

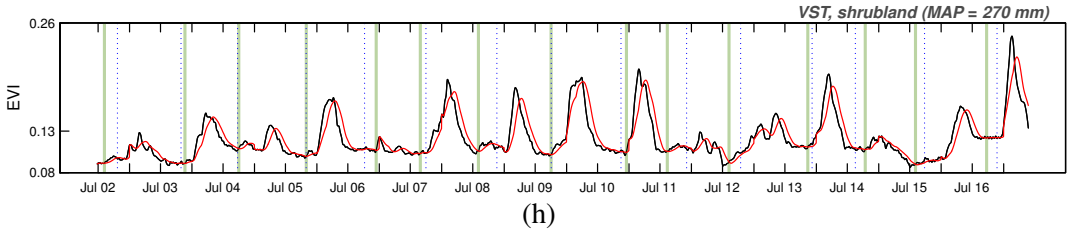

(h)

Figure A.1: **Fifteen-year time series of MODIS EVI (solid grey line) and TRMM rainfall (vertical grey bars)** for (a) *Maziba Bay Forest*, (b) *Sachinga Agricultural Station*, (c) *Pandamatenga Agricultural Station*, (d) *Maun Research Centre*, (e) *Sandveld Research Station*, (f) *Okwa River Crossing*, (g) *Tshane Tshane*, (h) *Vastrap Weapons Range*. Day of year is shown for green-up and rainfall onset in vertical green and blue line, respectively.